BioOne DIGITAL LIBRARY

The Neurocranium of Ekweeconfractus amorui gen. et sp. nov. (Hyaenodonta, Mammalia) and the Evolution of the Brain in Some Hyaenodontan Carnivores

Authors: Flink, Therese, Cote, Susanne, Rossie, James B., Kibii, Job M., and Werdelin, Lars

Source: Journal of Vertebrate Paleontology, 41(2)

Published By: The Society of Vertebrate Paleontology

URL: https://doi.org/10.1080/02724634.2021.1927748

The BioOne Digital Library (https://bioone.org/) provides worldwide distribution for more than 580 journals and eBooks from BioOne's community of over 150 nonprofit societies, research institutions, and university presses in the biological, ecological, and environmental sciences. The BioOne Digital Library encompasses the flagship aggregation BioOne Complete (https://bioone.org/subscribe), the BioOne Complete Archive (https://bioone.org/archive), and the BioOne eBooks program offerings ESA eBook Collection (https://bioone.org/esa-ebooks) and CSIRO Publishing BioSelect Collection (https://bioone.org/csiro-ebooks).

Your use of this PDF, the BioOne Digital Library, and all posted and associated content indicates your acceptance of BioOne's Terms of Use, available at www.bioone.org/terms-of-use.

Usage of BioOne Digital Library content is strictly limited to personal, educational, and non-commmercial use. Commercial inquiries or rights and permissions requests should be directed to the individual publisher as copyright holder.

BioOne is an innovative nonprofit that sees sustainable scholarly publishing as an inherently collaborative enterprise connecting authors, nonprofit publishers, academic institutions, research libraries, and research funders in the common goal of maximizing access to critical research.

Downloaded From: https://complete.bioone.org/journals/Journal-of-Vertebrate-Paleontology on 22 Mar 2025
Terms of Use: https://complete.bioone.org/terms-of-use

Journal of Vertebrate Paleontology e1927748 (16 pages)
Published with license by the Society of Vertebrate Paleontology
DOI: 10.1080/02724634.2021.1927748

ARTICLE

THE NEUROCRANIUM OF *EKWEECONFRACTUS AMORUI* GEN. ET SP. NOV. (HYAENODONTA, MAMMALIA) AND THE EVOLUTION OF THE BRAIN IN SOME HYAENODONTAN CARNIVORES

THERESE FLINK,[1,2] SUSANNE COTE,[3] JAMES B. ROSSIE,[4] JOB M. KIBII,[5] and LARS WERDELIN[2*]
[1]Department of Earth Sciences, Uppsala University, Villavägen 16, SE-752 36 Uppsala, Sweden;
[2]Department of Palaeobiology, Swedish Museum of Natural History, Box 50007, S-104 05 Stockholm, Sweden, therese.flink@nrm.se, lars.werdelin@nrm.se;
[3]Department of Anthropology and Archaeology, University of Calgary, 2500 University Drive NW, Calgary, Alberta T2N 1N4, Canada, scote@ucalgary.ca;
[4]Department of Anthropology, Stony Brook University, Stony Brook, New York 11794, U.S.A., james.rossie@stonybrook.edu;
[5]Department of Earth Sciences, National Museums of Kenya, P.O. BOX 40658, Nairobi 00100, Kenya, jkibii@museums.or.ke

ABSTRACT—We report on a nearly complete cranium of *Ekweeconfractus amorui* gen. et sp. nov. (Hyaenodonta, Teratodontinae), from the early Miocene of Moruorot, Kenya. The cranium is dorsoventrally compressed, but sufficiently intact to allow for digital reconstruction of the neurocranium, resulting in a digital endocast that gives us a first glimpse into teratodontine brain morphology. The virtual endocast is one of the most well preserved of any hyaenodont known to date, with many of the cranial nerves and blood vessels identifiable. Endocasts are known from only a handful of hyaenodont species and little work has been done on hyaenodont brains in recent decades. To better understand the evolution of the brain in these animals, we place the endocast of *E. amorui* gen. et sp. nov., as well as several other previously described endocasts, in the latest phylogenetic framework. This analysis suggests that the expansion of the neocortex occurred convergently in several clades of Hyaenodonta. Our study provides a basis for future research on brain evolution in Hyaenodonta.

http://zoobank.org/urn:lsid:zoobank.org:pub:DB6CBB7A-16B8-49A1-816F-BC7367033620

SUPPLEMENTAL DATA—Supplemental materials are available for this article for free at www.tandfonline.com/UJVP

Citation for this article: Flink, T., S. Cote, J. B. Rossie, J. M. Kibii, and L. Werdelin. 2021. The neurocranium of *Ekweeconfractus amorui* gen. et sp. nov. (Hyaenodonta, Mammalia) and the evolution of the brain in some hyaenodontan carnivores. Journal of Vertebrate Paleontology. DOI: 10.1080/02724634.2021.1927748

INTRODUCTION

The extinct order Hyaenodonta Van Valen, 1967, encompasses a wide range of carnivorous mammals from Europe, Africa, Asia and North America dating from the late Paleocene to the middle Miocene. Hyaenodonta is currently placed in the Superorder Ferae together with extant Carnivora and Pholidota (Flynn and Wesley-Hunt, 2005; Friscia and Van Valkenburgh, 2010; Solé et al., 2015a). The systematic affinities of Hyaenodonta are still widely debated, however (e.g., Spaulding et al., 2009; Borths et al., 2016), as are the phylogenetic relationships within the order (e.g., Rana et al., 2015; Borths et al., 2016; Borths and Stevens, 2019; Dubied et al., 2019).

Borths et al. (2016) used parsimony analysis, standard Bayesian inference and Bayesian tip-dating on a large sample of hyaenodont taxa in an attempt to resolve the phylogeny within the order. The analyses in Borths et al. (2016) suggested that the overwhelmingly African clade Teratodontinae is closely related to Hyainailouridae, a clade that, in turn, includes Hyainailourinae and Apterodontinae. These three subfamilies are united, together with a number of more restricted taxonomic groupings, in Hyainailouroidea, which includes the majority of the African hyaenodonts. Hyaenodontidae, which includes the subfamily Hyaenodontinae and a number of other taxa, was consistently placed separately from all Afro-Arabian taxa. Borths and Seiffert (2017), Borths and Stevens (2017), and Dubied et al. (2019) all used a modified version of the same matrix and added taxa and characters. The phylogeny in Dubied et al. (2019) unites Hyaenodontidae with Proviverrinae in Hyaenodontoidea.

The present study describes a new species of teratodontine, *Ekweeconfractus amorui* gen. et sp. nov., based on a newly found, crushed but nearly complete cranium from the early Miocene of Kenya. The cranium of *E. amorui*, gen. et sp. nov. was digitized using high resolution computed tomography scanning. The lack of weathering and plastic deformation of the cranium allowed for reconstruction of the neurocranium and creation of a digital cast of the cranial cavity. This endocast provides the first evidence of teratodontine brain morphology, filling a

*Corresponding author
© 2021, Therese Flink, Susanne Cote, James B. Rossie, Job M. Kibii, Lars Werdelin.
This is an Open Access article distributed under the terms of the Creative Commons Attribution-NonCommercial-NoDerivatives License (http://creativecommons.org/licenses/by-nc-nd/4.0/), which permits non-commercial re-use, distribution, and reproduction in any medium, provided the original work is properly cited, and is not altered, transformed, or built upon in any way.
Color versions of one or more of the figures in the article can be found online at www.tandfonline.com/ujvp.

Downloaded From: https://complete.bioone.org/journals/Journal-of-Vertebrate-Paleontology on 22 Mar 2025
Terms of Use: https://complete.bioone.org/terms-of-use

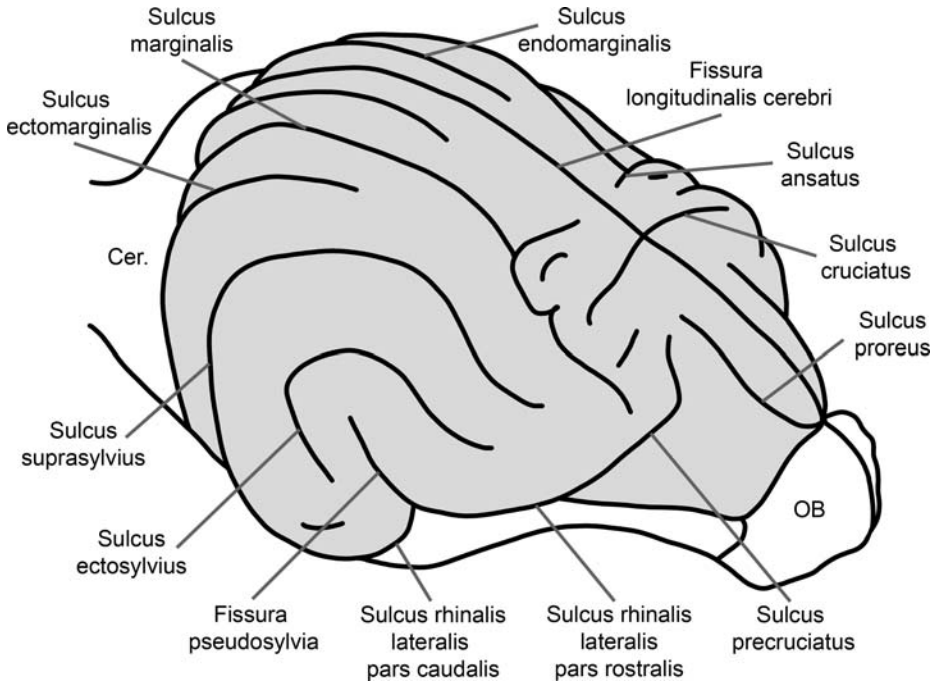

FIGURE 1. Sulci of the brain of the domestic dog, in anterodorsolateral view. Neocortex highlighted in gray. Drawing based on the illustration of an endocast in Lyras and Van der Geer (2003:fig. 1). **Abbreviations**: **cer**, cerebellum; **OB**, olfactory bulb.

large gap in our understanding of hyaenodont brain evolution. For the first time, endocasts spanning all major hyaenodont subfamilies can be placed in a phylogenetic context, furthering our understanding of the evolution of the brain in this group.

The study of the endocranium of fossil mammals originated with Cuvier (1804), who commented on a natural endocast of the brain of *Palaeotherium*, an Eocene relative of the horse. Gervais (1870) appears to have been the first to publish an endocast of a fossil carnivore and a few years later published several more. Subsequent study of mammalian endocasts has been intermittent, as summarized by Edinger (1975). Tilly Edinger is the most important figure in the study of paleoneurology, with many publications, including some on carnivores, such as a study of the Miocene mustelid *Pannonictis* (Edinger, 1931). Piveteau (1935, 1951, 1961) also published on a range of early carnivore taxa, including some hyaenodonts. Nevertheless, the most prominent student of the evolution of the carnivore brain was L. B. Radinsky, whose publications (e.g., Radinsky, 1969, 1973, 1975, 1977, 1978) laid the foundation for all subsequent study of the topic. Radinsky's work mainly concerned extant species of Carnivora, but he complemented this with natural endocasts of fossil carnivores where available. Combining extant and extinct taxa, Radinsky was able to draw some broad conclusions regarding brain evolution in (primarily) Canidae and Felidae, but also in early carnivores (Radinsky, 1969, 1973, 1975, 1977, 1978).

Radinsky (1977) compared a large number of endocasts of early carnivores, including several hyaenodonts. He found that over time brain size tended to increase relative to body size in these animals, but he found no evidence for earlier assumptions that the ancestors of extant carnivorans had larger brains than contemporaneous, now extinct, carnivores like hyaenodonts (Jerison, 1973). He also found that the relative size of the neocortex increased through time in both hyaenodonts and early carnivoramorphs. Neocortical expansion is also seen in many other groups of mammals and is a prime example of parallel evolution (e.g., Radinsky, 1977, 1978; Kaas, 2016; López-Torres et al., 2020).

The neocortex is a mammalian feature that is histologically different from the rest of the brain. It is delimited ventrally by the sulcus rhinalis, which is generally visible on endocranial casts. As the neocortex expands, it becomes more convoluted, i.e., more sulci appear. Larger brains therefore tend to have more convolutions and a greater volume of neocortical tissue relative to the total volume of the brain (e.g., Jerison, 1973; Finlay and Darlington, 1995). What determines the shape of the sulci is not fully understood, and there are several theories, including genetics (Bartley et al., 1997) and mechanical factors related to the shape and thickness of the cortex (Toro, 2012; Heuer and Toro, 2019).

In modern mammals, sulci have been shown to delimit different functional areas of the cortex, which means that enlargement of a certain gyrus may hint at a specific sensory specialization (e.g., Welker and Campos, 1963; Radinsky, 1968). Similar sulcal patterns in distantly related taxa are, however, not necessarily homologous. For example, Lyras (2009) showed that three subfamilies of canids followed highly convergent paths of brain evolution, and that the cruciate sulcus (Fig. 1) appeared as many as four times independently within Canidae. Endocast morphology can, nevertheless, provide phylogenetic information. Ahrens (2014) used geometric morphometrics and principal component analysis of endocast morphology in Procyonidae to test two differing phylogenetic hypotheses, one based on morphology and one based on molecular data. She found a significant phylogenetic signal in brain shape that supported the morphological phylogeny.

Although the carnivoran brain is relatively well researched, the same cannot be said of those of hyaenodonts or basal carnivoramorphs, owing largely to the lack of suitable material. Previous studies on hyaenodont endocrania are few and exclusively based on physical casts (Gervais, 1870; Filhol, 1877; Gaudry, 1878; Scott, 1888; Klinghardt, 1934; Piveteau, 1935, 1961; Savage, 1973; Radinsky, 1977; Lange-Badré, 1979; Saveliev and Lavrov, 2001, 2007) with the exception of the recent description of the endocast of *Proviverra typica* by Dubied et al. (2019) which is based on digital reconstruction from a

Downloaded From: https://complete.bioone.org/journals/Journal-of-Vertebrate-Paleontology on 22 Mar 2025
Terms of Use: https://complete.bioone.org/terms-of-use

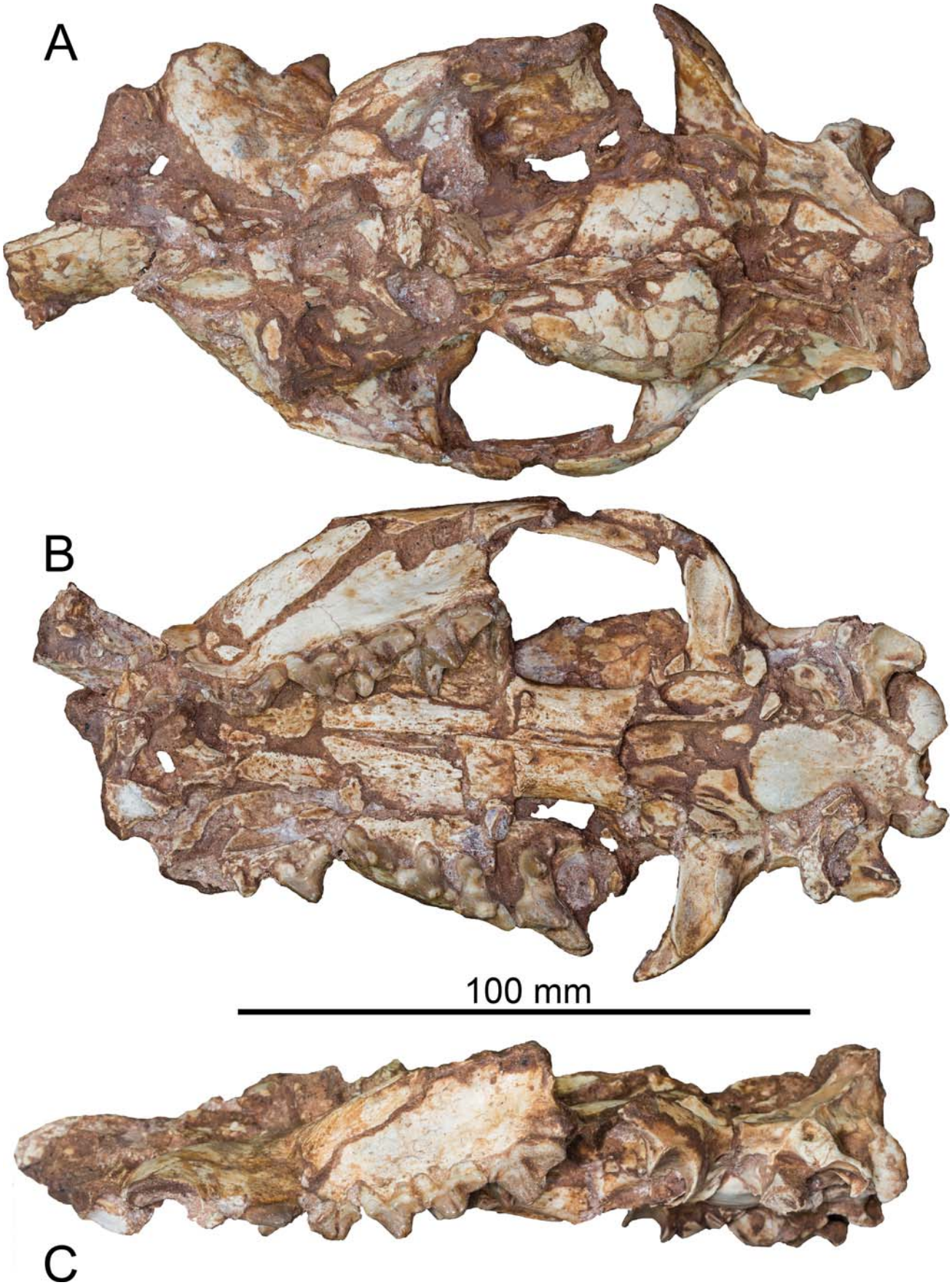

FIGURE 2. Photographs of the fossil holotype cranium, KNM-MO 64199, of *Ekweeconfractus amorui* gen. et sp. nov., in **A**, dorsal, **B**, ventral and **C**, left lateral view. **A** and **B** are reversed so that the snout faces to the left, for consistency with other figures.

Downloaded From: https://complete.bioone.org/journals/Journal-of-Vertebrate-Paleontology on 22 Mar 2025
Terms of Use: https://complete.bioone.org/terms-of-use

computed tomography (CT) scan. In the present study, the digital endocast of *Ekweeconfractus amorui* gen. et sp. nov., as well as several hyaenodont endocasts previously described, are placed in the latest phylogenetic framework in order to better understand the evolution of the brain in the different hyaenodont lineages.

GEOLOGICAL SETTING

The described specimen, KNM-MO 64199, consists of a nearly complete cranium (Fig. 2) from the early Miocene site Moruorot in Kenya. It was discovered in 2016 during excavations by the West Turkana Miocene Project. Moruorot lies within the Lothidok Formation west of Lake Turkana in northern Kenya (for detailed geological description, maps and stratigraphic sequence, see Arambourg, 1944; Boschetto et al., 1992) and is divided into two localities, Moruorot South and Moruorot North, located on the flanks of Moruorot Hill. The exposures include both the lower portion of the Kalodirr Member (the Kalodirr Tuffs), and the upper strata of the Moruorot Member. The new cranium was found at Moruorot South, in strata believed to fall within the lowest portion of the Kalodirr Member, near or intercalated among the Kalodirr Tuffs. There is at least one tuff exposed down-section from the excavation, and no tuffs are described in the Moruorot Member (Boschetto et al., 1992). The Kalodirr Tuffs are dated by a number of amphibole and biotite samples ranging from 17.3 ± 0.3 Ma to 17.7 ± 0.03 Ma, with a mean of 17.5 Ma (Boschetto et al., 1992). The age of the specimen is best regarded as within this range as well.

Despite the site being discovered in the 1930s (Arambourg, 1933), little work was done at Moruorot until the 1980s (Leakey et al., 2011). It is now one of the main sites being studied by the West Turkana Miocene Project (e.g., Rossie et al., 2012; Rossie and Cote, 2017). To date the site has yielded a wide variety of skeletal remains of mammals, including among others *Prodeinotherium*, *Cynelos*, *Afrosmilus*, *Ekweeconfractus amorui* gen. et sp. nov. (discussed herein), *Paraphiomys*, *Turkanatherium*, and a large number of artiodactyls including *Canthumeryx*, *Sivameryx*, *Kenyasus*, and *Diamantohyus*. The faunal list resembles other early Miocene sites in the region, but the artiodactyls most closely resemble those from the Hiwegi Formation at Rusinga Island (Drake et al., 1988; Cote et al., 2018). Notably, the three ape species found at Moruorot are endemic to the Turkana Basin. For a full faunal list, see Leakey et al. (2011).

The cranium of *E. amorui* gen. et sp. nov. was found in a fine-grained bed, associated with a skeleton of the primate *Simiolus*, as well as two currently unidentified carnivorans, a snake, and fragments of several smaller mammals. The fossils lay close to the top of a large overbank deposit, which was exposed for a long time, likely millennia, before being covered by another such deposit. The ape, snake, carnivorans, and *E. amorui* gen. et sp. nov. all share the same remarkably unweathered state of preservation. These are interspersed with remains of other taxa that are less complete and more weathered. The latter may have been exposed for a longer period of time on the same surface as the well-preserved specimens, or they may have originally been deposited in the older underlying paleosol and redeposited in the higher paleosol by bioturbation.

MATERIALS AND METHODS

Digital Reconstruction

The specimen was scanned using a Nikon Metrology XTH 225/320 LC dual source industrial computed tomography scanner at the Evolutionary Studies Institute, University of the Witwatersrand, South Africa. The scan parameters were 80 kV and 130 μA, and the voxel size was 0.0667 mm. The contrast between bone and sediment was good (Fig. 3), but because of the varying density of the bone and of the large number of high-density crystals in the sediment, the contrast was insufficient for automatic segmentation. The bone was therefore segmented out manually in Avizo 9.5.0 (ThermoFisher Scientific, Waltham, Massachusetts, U.S.A.). A preliminary reassembly (see Supplemental Data 1) was performed in Avizo to determine which bone fragments were identifiable and of use in the reconstruction. Those bone fragments that were identifiable were exported and reassembled in Blender 2.79b (blender.org). There was no plastic deformation of the bone. The medial and left parts of the cranium were reconstructed using both fragments from those sides and mirrored fragments from the right side in order to make it as complete as possible. The composite left side was then mirrored, and the mirrored part fitted against the medial parts of the cranium in order to make it complete. The cranial cavity of the reconstructed neurocranium was then segmented in Avizo. Due to the amount of missing bone, the cranial cavity had to be manually segmented. Where bone was missing, segmentation followed the curvature of the surrounding bone; these areas are shown in darker gray herein. More details about the reconstruction process, including fragment maps before and after reconstruction, are presented in Supplemental Data 1 and Figures S1, S2. The dorsal-most and rostral-most parts of the neurocranium were too fragmented and could not be reconstructed. On the endocast, these areas correspond to the dorsal part of the cerebellum, the fissura longitudinalis cerebri, the rostral-most part of the cerebrum and the olfactory bulbs. The majority of the cranial cavity could be reconstructed with confidence, with only narrow strips of missing bone in a few places. On the endocast, the major cerebral sulci are visible as well as the passages of the major nerves and blood vessels on the ventral side of the brain. The greatest degree of uncertainty is in the rostral part where the bone was more damaged and not all fragments fit together well. This is unlikely to affect the interpretation of the endocast significantly but may have slightly altered the general shape of the rostral-most cerebrum. The interpretation of the sulcal pattern should not be affected because all the sulci are preserved on bone fragments that fit well against several other fragments. Additionally, all sulci except the sulcus ectosylvius are preserved on bone fragments from both the left and right side of the cranium (see Supplemental Data 1, Fig. S2).

Raw scan data and 3D surface renderings of the endocast and neurocranium are available on MorphoSource through the following DOIs: CT image stack, https://doi.org/10.17602/M2/M166152; segmented neurocranium, https://doi.org/10.17602/M2/M166153; reconstructed neurocranium, https://doi.org/10.17602/M2/M166154; endocast, https://doi.org/10.17602/M2/M166155.

Measurements such as length, width, and height of the endocast were taken in Avizo. Because the olfactory bulbs could not be reconstructed, the total length of the endocast is that of only the cerebrum and cerebellum. The area of the neocortex could not be measured because only small sections of the sulcus rhinalis lateralis, which forms part of the boundary of the neocortex, were preserved.

The volume of the endocast was calculated in Avizo using the 'Label analysis' tool. This gave the volume in number of voxels, which, using the voxel size, was converted into milliliters (ml). Because the endocast is missing the olfactory bulbs and dorsal cerebellum, the volume is lower than the true brain volume. Known olfactory bulb sizes of *Hyaenodon horridus* and *Cynohyaenodon cayluxi* (Jerison, 1973) were used to estimate the volume of the missing olfactory bulbs in *E. amorui* gen. et sp. nov.

Body Mass Estimation

Because body mass regressions for Hyaenodonta and Carnivora are based on lower molar length, and the lower dentition

Downloaded From: https://complete.bioone.org/journals/Journal-of-Vertebrate-Paleontology on 22 Mar 2025
Terms of Use: https://complete.bioone.org/terms-of-use

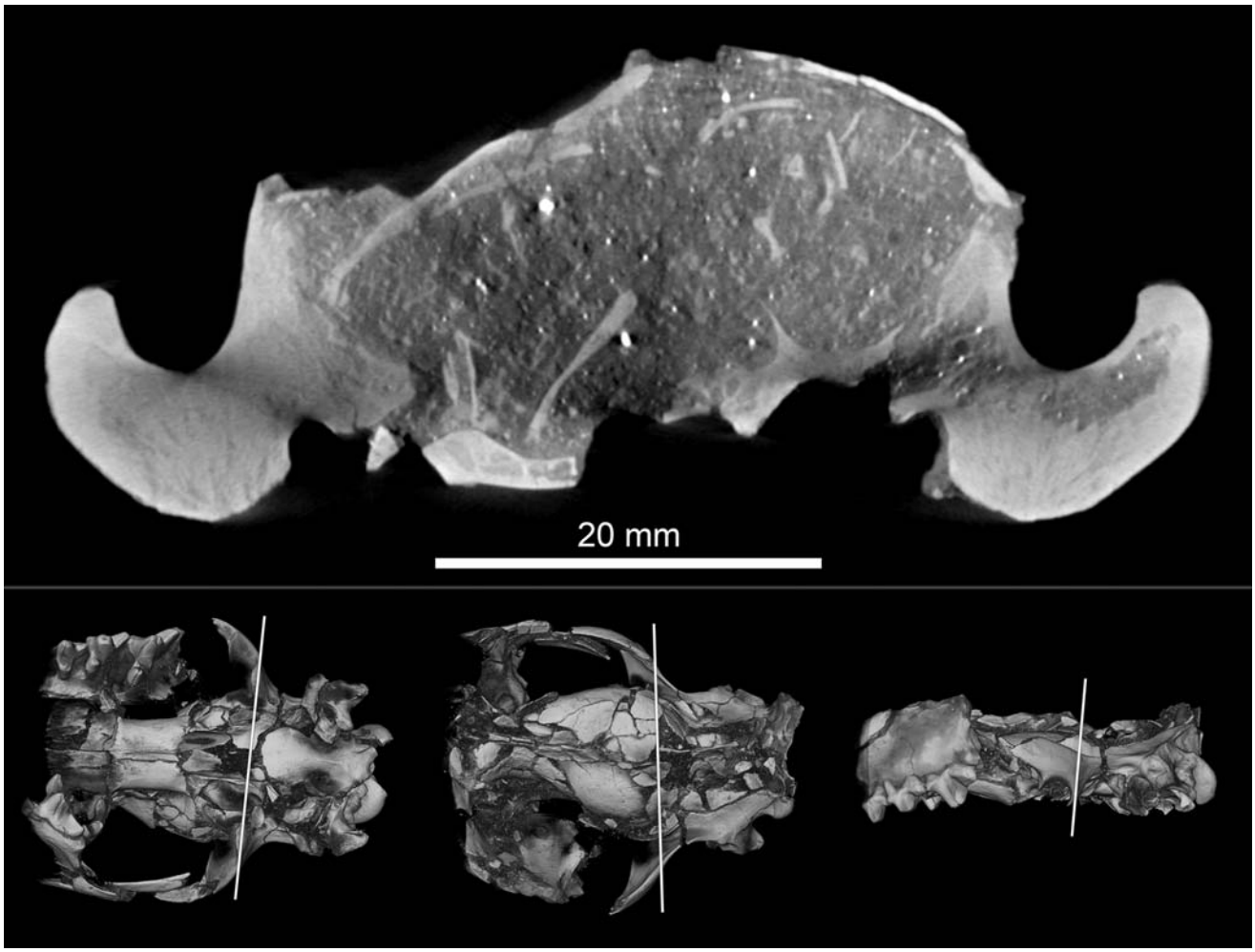

FIGURE 3. Cross-section of the scanned cranium KNM-MO 64199 of *Ekweeconfractus amorui* gen. et sp. nov. illustrating the bone to sediment contrast. The position of the cross-section on the cranium is indicated by a white line at the bottom of the figure, in ventral (left), dorsal (middle) and lateral (right) view.

of *Ekweeconfractus amorui* gen. et sp. nov. is not known, we used P4–M1 'upper occlusion length' (measured in Avizo) to estimate the length of m1 (Borths and Stevens, 2017:s1 appendix). The length of this tooth was then used to estimate body mass using the regression for carnivorans of 10–100 kg by Van Valkenburgh (1990). Body masses of *Megistotherium osteothlastes*, *Pterodon dasyuroides*, *Apterodon macrognathus*, *Tritemnodon agilis*, *Hyaenodon horridus*, *H. crucians*, *Cynohyaenodon cayluxi*, *Thinocyon velox* and *Vulpavus palustris* were taken from Radinsky (1977). Radinsky (1977) estimated the body masses of *H. horridus*, *H. crucians* and *T. agilis* based on body length and the body mass of the other taxa based on skull length. The body mass of *Proviverra typica* was estimated by Dubied et al. (2019) using average lower molar length (Morlo, 1999) of another individual of the same species. The body mass of *Paroxyaena pavlovi* is thought to be similar to that of *P. galliae* based on M1 size (Solé et al., 2015b). The body mass of *H. brachyrhynchus* is not currently known.

Encephalization Quotient

Because larger animals tend to have relatively smaller brains than smaller animals, comparing the brain to body ratio is usually not very informative. To better compare the relative brain sizes in different animals Jerison (1973) developed the encephalization quotient (EQ) which is the ratio of observed brain size to expected brain size in an animal of the observed body mass. This equation is: $EQ = E / 0.12P^{2/3}$, with E being the brain volume in ml and P the body mass in grams. Eisenberg (1981) composed a slightly different formula: $EQ = E / 0.055P^{0.74}$ (for all Mammalia). For comparative purposes both equations were used to calculate the EQ values of all species in this study for which endocast volume and body mass could be estimated. Where body masses were given in ranges in previous studies (e.g., Radinsky, 1977), both the minimum and maximum body mass was used to calculate a corresponding range of EQ values. Values mentioned in the text are those obtained using Jerison's equation unless otherwise specified, because this equation is used in previous studies on carnivore endocasts (e.g., Radinsky, 1977, 1978), allowing for easier comparison.

Comparison of Hyaenodont Endocasts

Radinsky (1977) compared a large number of endocasts of early carnivores, including several hyaenodonts and carnivoramorphs. He did not, however, look more closely at brain evolution within Hyaenodonta from a phylogenetic perspective. In this study, the hyaenodont endocasts previously described by Radinsky (1977)

Downloaded From: https://complete.bioone.org/journals/Journal-of-Vertebrate-Paleontology on 22 Mar 2025
Terms of Use: https://complete.bioone.org/terms-of-use

and others (Lange-Badré, 1979; Saveliev and Lavrov, 2007; Dubied et al., 2019) are placed in the latest phylogenetic framework (Borths et al., 2016; Borths and Stevens, 2019; Dubied et al., 2019) together with the endocast of *Ekweeconfractus amorui* gen. et sp. nov. reconstructed herein, in order to better understand the evolution of the brain in this group of animals and to provide a basis for future studies.

Comparative 3D surface renderings of several of these previously described endocasts were generously provided by George A. Lyras, National and Kapodistrian University of Athens, Greece. These included the hyaenodonts *Megistotherium osteothlastes* (NHMUK-M26515), *Pterodon dasyuroides* (MNHN, no number given; Piveteau, 1961), *Thinocyon velox* (FMNH PM 57146, cast of AMNH 12631), and *Hyaenodon crucians* (FMNH PM 58859), and the carnivoramorph *Vulpavus palustris* (FMNH PM 57174, cast of AMNH 19000). These models were created through laser scanning of the physical endocasts with a NextEnginge scanner (Santa Monica, California, U.S.A.). Models of the endocasts of *Proviverra typica* are available online (see Dubied et al., 2019). Our interpretations of these specimens and those of previous authors are compared in the Discussion.

Abbreviations, Repositories—**AMNH**, American Museum of Natural History, New York, U.S.A.; **FMNH**, Field Museum of Natural History, Chicago, U.S.A.; **KNM**, National Museums of Kenya, Nairobi, Kenya; **MNHN**, Muséum national d'Histoire naturelle, Paris, France; **NHMUK**, Natural History Museum (formerly BM[NH], British Museum [Natural History]), London, U.K.

Abbreviations, Measurements—**L**, length; **W**, width; **Wa**; anterior width including protocone; **Wbl**, blade width at mesial part of metastyle.

Terminology—Terminology for brain anatomy will follow the Nomina Anatomica Veterinaria (World Association of Veterinary Anatomists, 2017) for Carnivora.

SYSTEMATIC PALEONTOLOGY

Order HYAENODONTA Van Valen, 1967
Superfamily HYAINAILOUROIDEA Pilgrim, 1932 sensu Solé, Amson, Borths, Vidalenc, Morlo, and Bastl, 2015b
Family TERATODONTIDAE Savage, 1965
Subfamily TERATODONTINAE Savage, 1965 sensu Borths and Stevens, 2019
EKWEECONFRACTUS AMORUI gen. et sp. nov.

Holotype—A cranium with left P1–M2, right P3–M3, KNM-MO 64199 (Figs. 2, 4).

Hypodigm—Holotype only.

Etymology—From Turkana '*ekwee*', fox or jackal; Latin '*confractus*', broken, and Turkana '*amoru*', stone.

Occurrence—Moruorot South only.

Diagnosis—Teratodontinae of moderate size; paracone and metacone nearly indistinguishable on P4–M2; Cheek teeth increasing in size from P4 to M2; M1–M2 slender with elongated protocone neck and protocone set far mesial to parastyle; mesial face of P4–M2 concave; metastyle on M1–M2 long.

Description—The specimen is a complete but crushed cranium, lacking only parts of the premaxillae, part of the left zygomatic arch, with other minor fragments missing. The incisors and canines are missing, as are the right P1–2, right P3 (mesial end), and left M3, but the remaining cheek dentition is present and well preserved. The deformation has made it impossible to identify the cranial sutures with any certainty. The deformation is most severe anteriorly and across the nasals where much of the bone has been reduced to small fragments. The braincase, however, is largely intact and its bones, although separated, retain their three-dimensional shape with, as seen from CT scans, minimal distortion. Deformation is less severe on the ventral side due to it being relatively flat, such that large parts of the basioccipital and basisphenoid are relatively intact, as well as the temporal contribution to the zygomatic arch. The basicranium is also distorted and jumbled, but it can be observed that the basisphenoid is smooth and slightly vaulted and that the basioccipital has a central ridge.

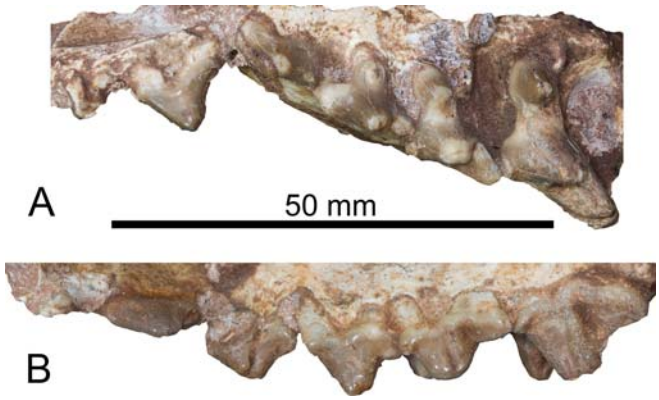

FIGURE 4. Photographs of the left upper dentition of KNM-MO 64199, *Ekweeconfractus amorui* gen. et sp. nov., in occlusal (**A**) and buccal view (**B**). The top image is reversed so that the snout faces to the left, for consistency with other figures.

The preserved cheek teeth are nearly undamaged (except for the right P3, as noted). There is some distortion of the tooth rows, such that the left side is seen in ventral (occlusal) view and the right side is seen in buccal view. The P4–M1 show some wear on the paracone/metacones and protocones but it is clear that the specimen was young because the M2 on either side is nearly unworn, although there is some damage to the right side protocone.

The description of the teeth will focus on the left side except as noted. The P1 is worn down to a small fragment but appears to have been two-rooted. The P2 is nearly symmetric in lateral view, with a straight mesial border and slightly concave distal one. The mesial end has a small mesiolingual protrusion whereas the distal end has a small cingulum. The P3 is very similar to P2 but is stouter and has a small distal accessory cusp and weak mesial and distal cingula. The P4 is a larger, stouter tooth than P2–3. It has a low parastyle with only a small mesial bump indicating a cusp. The protocone is well developed but low. The cusp apex is situated between the mesial end of the parastyle and the apex of the paracone/metacone. The latter two cusps are close and would not be distinguishable as two except for the small, ca. 1.5 mm long, groove on the buccal side where the fusion has not been complete (Fig. 4). The paracone is slightly the taller of the two cusps. The metastyle is short and low.

The M1 is slender. It has a very short parastyle with a small cusp at the mesial end. The protocone is large and stout and extends well mesial to the parastyle, reaching the level of the P4 paracone/metacone. It is nearly equally wide throughout its length. The paracone/metacone is large and tall. Due to wear the distinction between paracone and metacone cannot clearly be seen in occlusal view. In buccal view it can be seen that the two cusps are fused throughout their length but there is a groove on the buccal side that extends from the apex to the basal swelling of the tooth, i.e., fusion is less complete in this tooth than in P4. The metastyle is short but trenchant with a small lingual wear facet.

Downloaded From: https://complete.bioone.org/journals/Journal-of-Vertebrate-Paleontology on 22 Mar 2025
Terms of Use: https://complete.bioone.org/terms-of-use

The M2 is similar in general outline to the M1 but is larger. There is almost no parastyle and the paracone reaches nearly to the mesiobuccal corner of the tooth. The protocone is large and, like that of the M1, reaches to the level of the paracone/metacone of the tooth in front. There is a distinct neck leading to a wide and tall protocone cusp. The paracone and metacone are fused in this tooth as well, and like in M1 the buccal groove reaches to the basal swelling of the tooth. The metastyle is long and trenchant.

The M3 is a mesiodistally short but buccolingually wide tooth, nearly as wide as the distance from the M2 paracone to the distal end of that tooth. Its cusp pattern is unclear but it cannot be determined if this is because of wear or breakage.

Measurements: LP2 10.0; WP2 4.5; LP3 10.8; WP3 5.6; LP4 10.6; WaP4 8.2; WblP4 5.0; LM1 12.4; WaM1 10.3; WblM1 6.2; LM2 15.7; WaM2 14.8; WblM2 7.0.

Phylogenetic Position of *Ekweeconfractus amorui*—The phylogeny of Hyaenodonta has been the subject of a series of studies in the past decade (Solé et al., 2014; Solé et al., 2015b; Borths et al., 2016; Borths and Seiffert, 2017; Borths and Stevens, 2017, 2019; Dubied et al., 2019). Our object herein has not been to establish a new phylogeny and, in view of the cited ongoing work, we have not attempted an independent assessment of hyaenodont phylogeny. Instead, we have used the data matrix and phylogeny from Borths and Stevens (2017:s3 Dataset and s1 tree), coded *E. amorui* gen. et sp. nov. for the available characters (see Supplemental Data 2), and placed it in the most parsimonious position using the pre-existing phylogeny as a constraint. This was done in TNT (Goloboff et al., 2008) and then checked manually in Mesquite 3.6 1(Maddison and Maddison, 2019). This resulted in a single most parsimonious position for *E. amorui* gen. et sp. nov. at Node T49 in Borths and Stevens (2017), more derived than *Pakakali* and less derived than *Glibzegdouia* (see Figs. 5 and S3). The precision of this position in the phylogeny may be questioned, but of importance here is that *E. amorui* gen. et sp. nov. by this account represents a teratodontine and it will be discussed as such below.

Differential Diagnosis—This differential diagnosis is based on the phylogenetic position of *E. amorui* gen. et sp. nov. established above and the new species is therefore compared with taxa within Teratodontinae that are represented by cranial and/or upper dentition material. The relevant genera are therefore *Indohyaenodon*, *Anasinopa*, *Brychotherium*, *Dissopsalis*, *Furodon*, *Glibzegdouia*, *Masrasector*, *Teratodon*, and *Pakakali* (Savage, 1965; Simons and Gingerich, 1974; Crochet et al., 1990; Crochet et al., 2001; Bajpai et al., 2009; Solé et al., 2014; Borths et al., 2016; Borths and Seiffert 2017; Borths and Stevens 2017). Of these genera, *Furodon*, *Glibzegdouia*, and *Indohyaenodon* are early Eocene in age, *Brychotherium* is late Eocene, *Masrasector* late Eocene to early Oligocene, *Pakakali* late Oligocene, *Teratodon* early Miocene, and *Anasinopa* and *Dissopsalis* early to middle Miocene.

Anasinopa leakeyi and *Dissopsalis pyroclasticus* are similar to each other in many respects, although *D. pyroclasticus* is the larger of the two, and they can be treated together. In general proportions and size *E. amorui* gen. et sp. nov. is closely similar to *A. leakeyi*, whereas *D. pyroclasticus* is somewhat larger and also interpreted to be somewhat more hypercarnivorous. In detailed molar morphology there is one character that clearly sets *E. amorui* gen. et sp. nov. apart from both *A. leakeyi* and *D. pyroclasticus.* The M1 and M2 of both of the latter taxa have the paracone and metacone set well apart, with the paracone close to the mesiolingual end of the tooth. In *E. amorui* gen. et sp. nov., on the other hand, the paracone and metacone are completely fused in both M1 and M2 from crown to root (Fig. 4). The relative position of these cusps has been shown to be an important character in hyaenodont evolution (Borths and Seiffert, 2017) and the difference between the taxa under scrutiny here differentiates *E. amorui* gen. et sp. nov. from both *A. leakeyi* and *D. pyroclasticus.*

Ekweeconfractus amorui gen. et sp. nov. can be differentiated from *Brychotherium ephalmos* on the basis of the larger size of the former. Other dental characters differentiating the two include the less fused M1–M2 paracone and metacone of *Brychotherium* and the less anteriorly extended protocones of those teeth (Borths et al., 2016). Further, the P4 of *Brychotherium* is a nearly equilateral triangle with an almost straight mesial margin, whereas the P4 of *E. amorui* gen. et sp. nov. is longer than wide and has a mesial margin that is deeply excavated.

Furodon crocheti is known from several lower dentition specimens, but the upper dentition is represented by only two M1s (Solé et al., 2014). These can be differentiated from the M1 of *E. amorui* gen. et sp. nov. on the basis of their partly fused but well differentiated paracone and metacone that are set at an

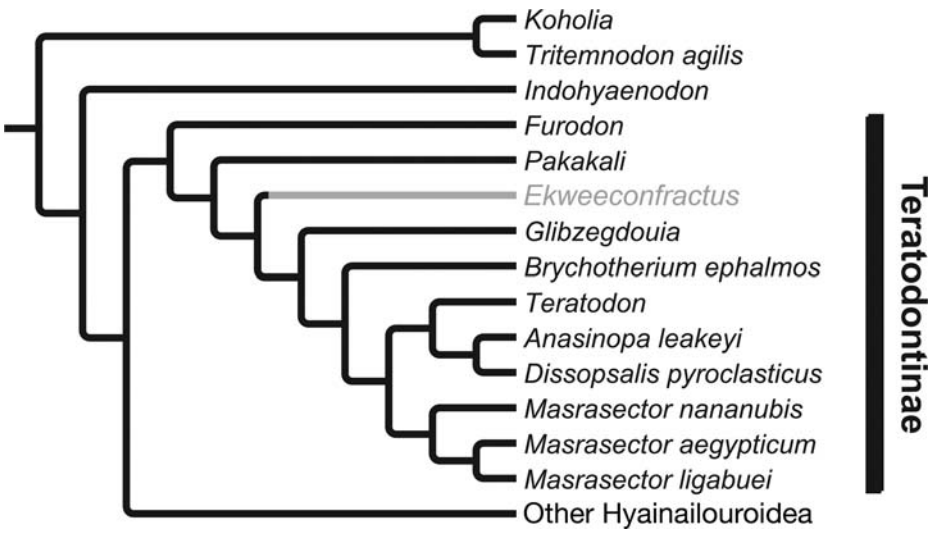

FIGURE 5. Extract of part of the phylogeny of Hyaenodonta from Borths and Stevens (2017) with *Ekweeconfractus amorui* gen. et sp. nov. in the most parsimonious position and the rest of the tree topology constrained. Full tree shown in Figure S3.

Downloaded From: https://complete.bioone.org/journals/Journal-of-Vertebrate-Paleontology on 22 Mar 2025
Terms of Use: https://complete.bioone.org/terms-of-use

angle of more than 45° to the buccal margin of the tooth. In *E. amorui* gen et sp. nov. the metacone and protocone apices are nearly indistinguishable, but are set at a much smaller angle to the buccal margin.

Glibzegdouia tabelbalaensis is differentiated from *E. amorui* gen. et sp. nov. by smaller size and by the paracone and metacone of M2 being entirely separate (Solé et al., 2014).

Masrasector spp. differ from *E. amorui* gen. et sp. nov. in the same characteristics as *Glibzegdouia*, but also (at least *M. nananubis*) in the proportions of P4–M2, which in *Masrasector* are nearly as wide as they are long, whereas in *E. amorui* gen. et sp. nov. they are mesiodistally elongated.

Ekweeconfractus amorui gen. et sp. nov. can be differentiated from *Teratodon spekei* on the basis of the very short and wide P4–M2 of the latter, as well as its clearly differentiated M2 paracone and protocone, P4 larger than M1, and specialized premolars.

Indohyaenodon raoi differs from *E. amorui* gen. et sp. nov. in size. The M2 of *I. raoi* is significantly less than half the length of that of *E. amorui* gen. et sp. nov. It also differs in the morphology of the tooth row. In *I. raoi* P4–M2 are very similar in length, whereas in *E. amorui* gen. et sp. nov. there is a gradual increase in length from P4 to M2. In addition, the paracone and metacone of *I. raoi* are more separated from each other than they are in *E. amorui* gen. et sp. nov.

Pakakali rukwaensis is known only from a juvenile maxillary fragment, and therefore there is no overlapping morphology to compare. We differentiate *P. rukwaensis* from *E. amorui* gen. et sp. nov. on the basis of size. Borths and Stevens (2017) calculated the m1 length of *P. rukwaensis* to be 8.3 mm. Our calculations of m1 length in *E. amorui* gen. et sp. nov. are given below as ca. 12 mm. This translates to a body mass for *P. rukwaensis* of approximately half that of *E. amorui* gen. et sp. nov. and this seems to be an excessive size difference even taking into account the sample size of N = 1 for both taxa.

RESULTS

Description of the Endocast

The cerebrum of *Ekweeconfractus amorui*, gen. et sp. nov. (Figs. 6, 7) is drop shaped in dorsal view with its widest point near the caudal end, above the piriform lobe. It is highest above the piriform lobe and tapers rostrally. The maximum width and height of the cerebrum are 38.3 mm and 31.3 mm respectively. The length of the endocast from the caudal end of

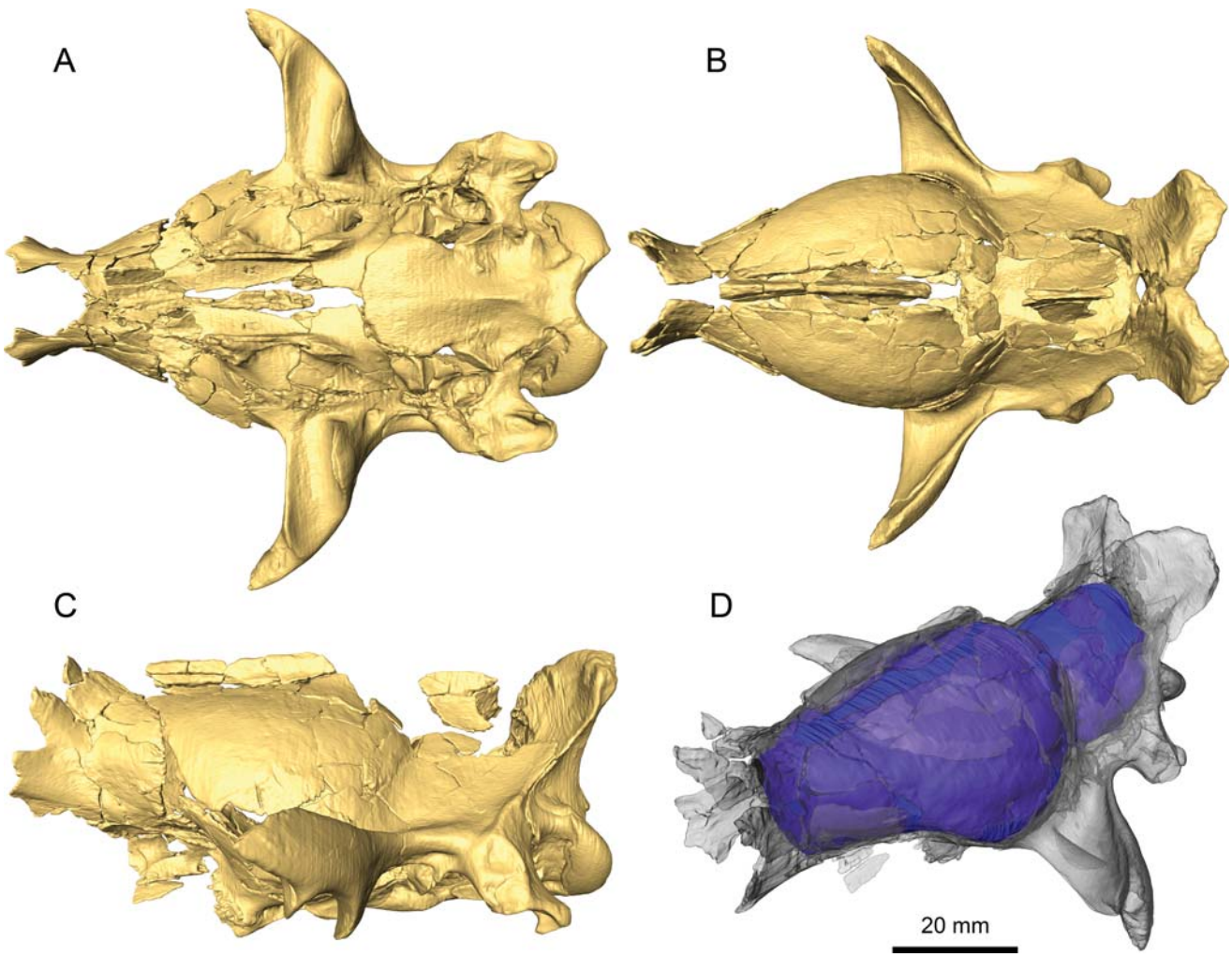

FIGURE 6. Digital reconstruction of the neurocranium of KNM-MO 64199, *Ekweeconfractus amorui* gen. et sp. nov., in **A**, ventral, **B,** dorsal, **C**, lateral, and **D**, anterodorsolateral view, with the cranium semi-transparent and the endocast shown within it. The apparent heart-shape of the dorsal part of the occiput is a result of mirroring of a broken bone fragment, where the dorsal-most part of the occiput is missing.

Downloaded From: https://complete.bioone.org/journals/Journal-of-Vertebrate-Paleontology on 22 Mar 2025
Terms of Use: https://complete.bioone.org/terms-of-use

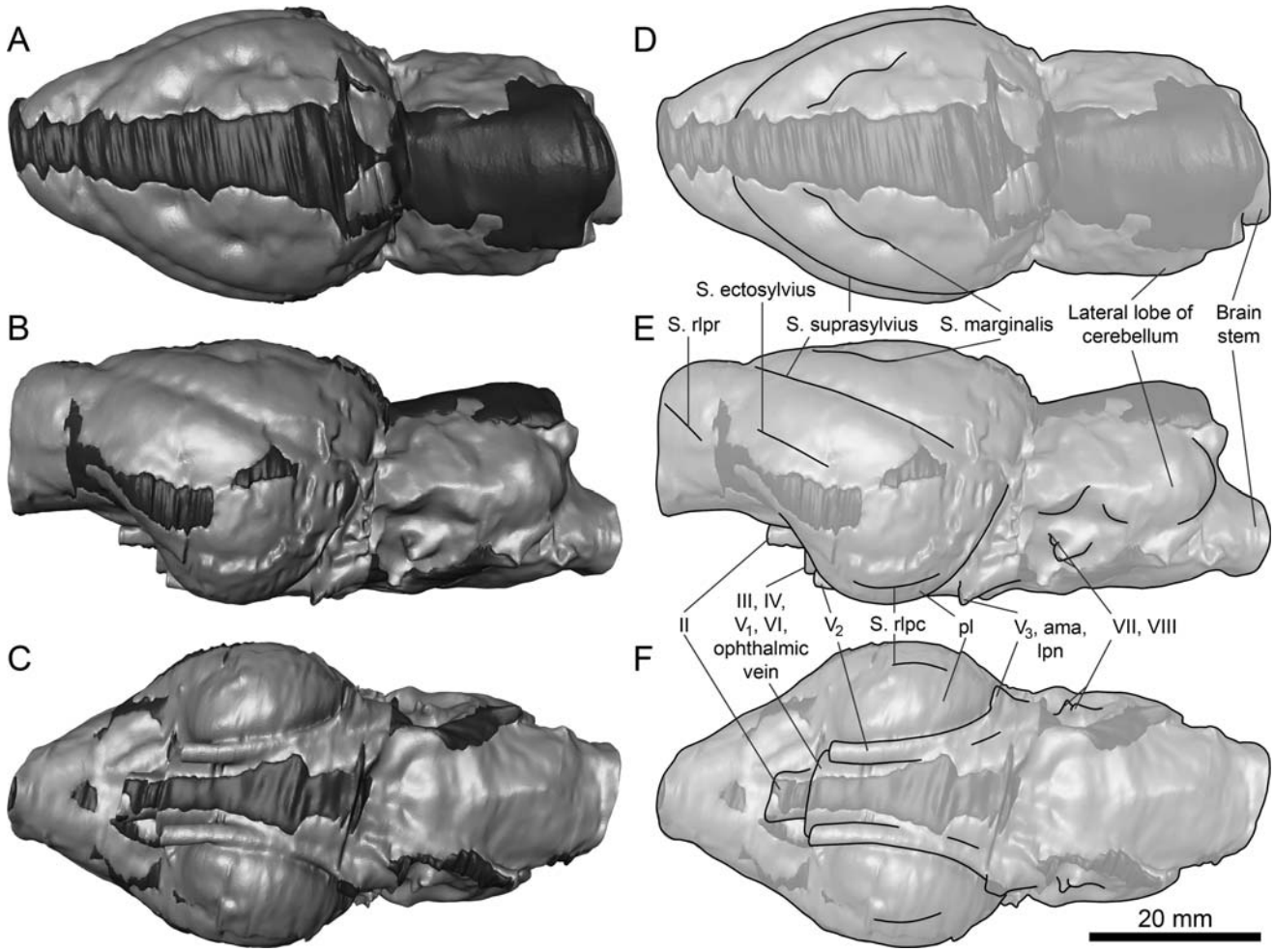

FIGURE 7. Digital endocast of *Ekweeconfractus amorui* gen. et sp. nov. (KNM-MO 64199), in **A**, **D**, dorsal, **B**, **E**, lateral and **C**, **F**, ventral view. **D**–**F** are drawings highlighting the major features. The areas shown in darker gray indicate where bone surrounding the endocast was missing. **Abbreviations**: **ama**, accessory meningeal artery; **lpn**, lesser petrosal nerve; **pl**, piriform lobe; **S**, sulcus; **S. rlpc**, sulcus rhinalis lateralis pars caudalis; **S. rlpr**, sulcus rhinalis lateralis pars rostralis; **II**–**VIII** refer to cranial nerves.

the cerebellum to the anterior end of the endocast (i.e., the rostral end of the cerebrum) is 68.6 mm. The lengths of the cerebrum and cerebellum are 45.5 mm and 23.1 mm respectively. The maximum width of the cerebellum is 28.5 mm, but the height is unclear because the dorsal-most part could not be reconstructed (Figs. 6, 7).

The ventral-most sulcus on the cerebrum is very faint, and partly obstructed by artifacts caused by the fragmented bone. Only the caudal-most and rostral-most parts of the sulcus are preserved; yet it is clearly a sulcus because it is not aligned with the edges of any bone fragments and is visible on the inside of the corresponding bone fragments on both the left and right side of the cranium (a comparison between the sulcal pattern on the endocast and on the bone fragments of the reconstructed cranium is available in Supplemental Data 1 and Fig. S2). This sulcus is positioned far ventrally on the cerebrum and appears to extend to the rostrodorsal end of the endocast (Fig. 7). This suggests that it is the sulcus rhinalis lateralis. Because the dorsal midline and rostral-most section of the endocast could not be reconstructed, the rostrocaudal expansion of the neocortex and the morphology of the olfactory bulbs remain unknown.

The second most ventral sulcus is faint, and difficult to discern in a still image, yet is clearly visible on the endocast in lateral view when shifting it up and down. It is visible on the inside of the large bone fragment from the left side of the cranium (see Supplemental Data 1, Fig. S2) that has also preserved the two additional sulci described below, but not on any fragment from the right side. This sulcus has its caudal section near the widest point of the cerebrum and is not visible in dorsal or ventral view. It is straight in lateral view and points rostrodorsally, so that it is nearly parallel with the sulcus rhinalis. The position of this sulcus corresponds most closely to the sulcus ectosylvius of carnivorans.

There is a very prominent neocortical sulcus (Fig. 7A, B, D, E) parallel to the sulcus ectosylvius, which is similar to the sulcus suprasylvius in carnivorans. This sulcus extends from near the caudal end of the cerebrum and curves medially to reach the fissura longitudinalis cerebri. More dorsally, there is a smaller sulcus (Fig. 7A, B, D, E) which is similar in position to the sulcus marginalis of carnivorans. This sulcus consists of two distinct dimples with a shallow furrow between them that continues caudal to the dimples. In dorsal aspect, both sulci appear to curve medially along their full length. Both of these sulci are preserved

Downloaded From: https://complete.bioone.org/journals/Journal-of-Vertebrate-Paleontology on 22 Mar 2025
Terms of Use: https://complete.bioone.org/terms-of-use

on bone fragments of both left and right sides of the cranium (see Supplemental Data 1, Fig. S2).

The cerebellum is square and noticeably narrower than the cerebrum, with relatively small hemispheres (Fig. 7A, D). The dorsal region, including the vermis, could not be reconstructed, and the degree of midbrain exposure is unclear.

Casts of the passages of several of the cranial nerves and blood vessels are preserved on the ventral side of the endocast (Fig. 7C, F). At the rostral end of the cerebellum there are two small lateral extensions which are here interpreted to be for the vestibulocochlear nerve or cranial nerve (CN) VIII, as well as the facial nerve (CN VII). Rostral to this is the cast of the foramen ovale, which houses the mandibular nerve (CN V_3), accessory meningeal artery, and lesser petrosal nerve. The maxillary nerve (CN V_2) lies along the ventral border of the piriform lobe. Medial and parallel to this is the cast of the fissura orbitalis, which houses the oculomotor nerve (CN III), trochlear nerve (CN IV), ophthalmic nerve (CN V_1), abducens nerve (CN VI), and ophthalmic vein. Next to this, along the midline of the ventral side of the brain, lies the optic nerve (CN II) as indicated by the cast of the canalis opticus. The region of the hypophysis is not preserved.

Body Mass and Encephalization Quotient

The body mass of *E. amorui* gen. et sp. nov. was estimated based on P4–M1 'upper occlusion length' which was measured at 11.67 mm on the left side and 11.54 mm on the right side. This corresponds to a first lower molar length of 12.11 mm and 11.98 mm, respectively (Borths and Stevens, 2017:appendix s1). This in turn leads to an estimated body mass of 15.6–15.8 kg for *E. amorui* gen. et sp. nov. As pointed out by Borths and Stevens (2017:appendix s1), the use of m1 length in body mass estimates for Hyaenodonta is likely to produce slight underestimates.

The endocast volume was measured at 37.6 ml. The olfactory bulb sizes of *Hyaenodon horridus* and *Cynohyaenodon cayluxi* (Jerison, 1973) suggest that the olfactory bulbs make up 6.0–8.2% of the total brain volume in hyaenodonts. Assuming a similar relative olfactory bulb size in *E. amorui* gen. et sp. nov., the volume the endocast plus olfactory bulbs would be 40.0–41.0 ml. This value is likely still a slight underestimate, however, because of the missing parts of the dorsal cerebellum. With an estimated body mass of 15.6–15.8 kg, that gives *E. amorui* gen. et sp. nov. an EQ of 0.53–0.55 or 0.57–0.59 using the Jerison (1973) and Eisenberg (1981) equation, respectively. The EQ values based on the endocast volume without olfactory bulbs are 0.50 and 0.53–0.54 respectively.

Comparison with Other Hyaenodonta

The elongated brain with a drop-shaped cerebrum observed in *E. amorui* gen. et sp. nov. is typical of known hyaenodont endocasts. In comparison with previously described hyaenodont endocasts, *E. amorui* gen. et sp. nov. appears to show a high degree of neocortical expansion. This is indicated by the relatively low position of the sulcus rhinalis, compared with many other hyaenodonts, such as *Tritemnodon agilis*, *Thinocyon velox*, *Hyaenodon crucians*, and *Pterodon dasyuroides* (Radinsky, 1977). The position of the sulcus rhinalis in *E. amorui* gen. et sp. nov. is more similar to that of *Megistotherium osteothlastes* (Radinsky, 1977) and *Paroxyaena pavlovi* (Saveliev and Lavrov, 2007). The gyrification of the neocortex in *E. amorui* gen. et sp. nov. is also fairly derived, as indicated by the presence of the sulcus suprasylvius and the sulcus ectosylvius, which are not present in, e.g., *T. agilis* and *T. velox* (Radinsky, 1977). *Ekweeconfractus amorui* gen. et sp. nov. is unusual, however, in its relatively narrow cerebellum, compared to the cerebrum, which is markedly wider. In some hyaenodonts, such as *T. agilis* and *M. osteothlastes*, the cerebellum is wider than the cerebrum (Radinsky, 1977), and in many others the two are of approximately equal width. The cerebellum of *Proviverra typica* is slightly narrower than the cerebrum (Dubied et al., 2019), but not to the extent seen in *E. amorui* gen. et sp. nov. The greater relative width of the cerebrum in *E. amorui* gen. et sp. nov. is not likely to have been caused by the reconstruction process. The fragments from the left side of the cranium which delimit the lateral parts of the endocast, fit well together and largely overlap with corresponding mirrored fragments from the right side.

The casts of the passages of nerves and veins on the ventral side of the endocast of *E. amorui* gen. et sp. nov. represent the typical mammalian condition and are similar to those of other hyaenodonts. In the endocasts of *E. amorui* gen. et sp. nov. and the other hyainailouroideans studied, *P. dasyuroides* and *M. osteothlastes*, the foramen rotundum (CN V_2) appears relatively well separated from the fissura orbitalis (CN III, IV, V_1 and VI) so that the former is positioned caudal to the latter. By comparison, in *P. typica* (Dubied et al., 2019), *C. cayluxi* (Lange-Badré, 1979) and *H. brachyrhynchus* (Lange-Badré, 1979), these passages appear to exit close together or even to be fused. The ventral side of the endocast of *P. pavlovi* is not exposed (Saveliev and Lavrov, 2007), but Lavrov (2007) noted the fusion of the fissura orbitalis and the foramen rotundum when describing the cranium.

The EQ appears relatively constant within Hyaenodonta, with an average of 0.57 (standard deviation 0.15). The only species to fall above the range of one standard deviation from the average are *H. crucians* and *H. horridus* with EQs of 0.88 and 0.78, respectively. *P. typica*, with an estimated EQ of 0.38, falls more than one standard deviation below the average, though as clarified below, the EQ of this species is underestimated due to the incompleteness of the endocast. The EQ of 0.53–0.55 for *E. amorui* gen. et sp. nov. is in the lower range of EQ values for hyaenodonts, yet not far from the average (Table 1) considering that the value is thought to be underestimated.

DISCUSSION

Conflicting Interpretations in the Literature on Hyaenodont Endocasts

An endocast of *Proviverra typica* was recently described by Dubied et al. (2019). They described a damaged cranium broken into two parts and provided digital casts of the endocranial space of each part. The caudal part of the endocast represents the cerebellum and most of the cerebrum, while the rostral part represents the olfactory bulbs and turbinals. A small part of the brain, connecting the cerebrum to the olfactory bulbs, is missing in their specimen. They calculated a volume of 13.45 ml for the caudal part of the endocast and the olfactory bulbs, a volume that would be extraordinarily large for an animal of that size and geological age. Additionally, given the length and width of the endocast listed in the text (measurements which agree well with the figures), the endocast would have had to be several times higher than wide to reach that volume. To provide an alternative volume estimate for the endocast, we used the method of graphic double integration (Jerison, 1969, 1973), measuring the width and height at each millimeter along the length of the endocast from their figure (Dubied et al., 2019:fig. 4) in dorsal and lateral view respectively. The volume of the caudal part of the endocast and that of the olfactory bulbs were calculated separately and then added together, providing a total volume of 2.91 ml. This method has proven to be very accurate (Jerison, 1969, 1973), although errors may occur when taking measurements from a figure that was never intended

Downloaded From: https://complete.bioone.org/journals/Journal-of-Vertebrate-Paleontology on 22 Mar 2025
Terms of Use: https://complete.bioone.org/terms-of-use

TABLE 1. Estimated body masses, endocast volumes, EQs and stratigraphical distributions of the taxa compared herein, arranged by descending age. Values indicated by asterisks are underestimates. Body mass estimates and endocast volumes are from Radinsky (1977), Saveliev and Lavrov (2007) and Dubied et al. (2019), except for the endocast volume of *P. typica* which was estimated herein, and all data regarding *E. amorui* gen. et sp. nov. References for stratigraphical ranges are listed in Supplemental Data 1.

Species	Stratigraphical distribution	Body mass (kg)	Endocast volume (ml)	EQ range (Jerison, 1973)	EQ range (Eisenberg, 1981)
Thinocyon velox	Early to middle Eocene	0.985–1.31	6	0.42–0.51	0.54–0.66
Tritemnodon agilis	Early to middle Eocene	8.89	26	0.50	0.57
Proviverra typica	Middle Eocene	0.500	2.91*	0.38*	0.53*
Cynohyaenodon cayluxi	Middle to late Eocene	2.51–3.47	12	0.44–0.54	0.52–0.66
Paroxyaena pavlovi	Late Eocene	46.7	70	0.45	0.45
Pterodon dasyuroides	Late Eocene	25.7–35.4	60	0.46–0.57	0.46–0.60
Hyaenodon crucians	Late Eocene to early Oligocene	9.41	47	0.88	0.98
Hyaenodon horridus	Late Eocene to early Oligocene	49.2	125	0.78	0.77
Apterodon macrognathus	Early Oligocene	25.7–35.4	70	0.59–0.73	0.59–0.75
Ekweeconfractus amorui gen. et sp. nov.	Early Miocene	15.6–15.8*	40.0–41.0*	0.53-0.55	0.57–0.59
Megistotherium osteothlastes	Early to middle Miocene	313–432	335	0.49–0.61	0.41–0.52
Vulpavus palustris	Early to middle Eocene	2.14–2.85	10.6	0.44–0.53	0.53–0.66

for that purpose. This endocast volume gives an EQ of 0.38, which is quite low for a hyaenodont. This is to be expected as the endocast is incomplete and the volume and EQ therefore underestimated.

In the description of the endocast Dubied et al. (2019) identified a single neocortical sulcus, the lateral sulcus (sulcus marginalis herein), which is prominent. In their comparison to other hyaenodonts, however, they also mention a sulcus suprasylvius, which they have highlighted in their drawing of the endocast in their comparative figure (Dubied et al., 2019:fig. 6). We have examined the 3D rendering of the endocast of *P. typica* that is available online. Its cerebral morphology is very similar to that of *Cynohyaenodon cayluxi* (e.g., Piveteau, 1961; Radinsky, 1977, Lange-Badré, 1979). We therefore suggest that what Dubied et al. (2019) interpreted as the sulcus suprasylvius in *P. typica* is in fact the sulcus rhinalis. This interpretation is supported by the amount of exposed midbrain, which suggests a low degree of neocortical expansion. Finally, the small sulcus (sulcus presylvius herein) branching off dorsally from the sulcus rhinalis lateralis pars rostralis in *C. cayluxi* (Radinsky, 1977) is present also in *P. typica*, but is most visible on the left hemisphere due to the damage to that area on the right hemisphere.

Cynohyaenodon cayluxi is represented by a well-preserved natural endocast which has been described and discussed by a number of authors (Filhol, 1877; Gaudry, 1878; Piveteau, 1961; Russel and Sigogneau, 1965; Radinsky, 1977; Lange-Badré, 1979), yielding several conflicting interpretations. Russel and Sigogneau (1965) suggested the presence of a weak sulcus suprasylvius, but this was disputed by Lange-Badré (1979). They agreed, however, regarding the presence of a fissura pseudosylvia (sylvian fossa in the latter publication). This fissura pseudosylvia was not mentioned by Radinsky (1977), who instead noted a small rostromedially oriented sulcus (sulcus presylvius herein) arising from the sulcus rhinalis lateralis pars rostralis. This sulcus was interpreted as the rostral-most part of the sulcus rhinalis by Piveteau (1961), an error which was corrected by Lange-Badré (1979). We have not had access to this specimen but choose to follow the interpretation by Radinsky (1977) because it appears to agree best with the original illustration in Filhol (1877:pl-I, figs. 199–202) and photographs in Lange-Badré (1979:pl. III) as well as with the similar endocast of *P. typica* discussed above.

Hyaenodon is the only hyaenodontan genus for which endocasts of several species are described, though the taxonomic assignments of the endocasts of *H. leptorhynchus* by Gervais (1870) and *Hyaenodon sp*. by Klinghardt (1934) were disputed by Scott (1888), Piveteau (1961), Radinsky (1977) and Lange-Badré (1979). An endocast of the cerebrum of *H. crucians* was figured by Leidy (1869) and described by Scott (1888). Radinsky (1977) further provided a latex cast of the left side of the cranial cavity of *H. crucians*. We have examined a digital rendering of this endocast and in addition to the two major sulci identified by Radinsky (sulcus marginalis and sulcus suprasylvius herein), we identify a faint sulcus ectosylvius parallel to the sulcus rhinalis and a sulcus endomarginalis parallel to the fissura longitudinalis cerebri. There is also a small depression emanating from the fissura longitudinalis cerebri in a similar place to the sulcus cruciatus in *H. brachyrhynchus* (Lange-Badré, 1979).

Scott (1888) described an endocast of *H. horridus*, and Radinsky (1977) described several more. Saveliev and Lavrov (2001) redescribed (as *Neohyaenodon horridus*) one of the endocasts previously included in the description by Radinsky (1977), but with major differences in interpretation. They provided photographs of the endocast and, based on these, it is our interpretation that Radinsky's description was essentially correct, and that the cerebral morphology of *H. horridus* is similar to that of *H. crucians* and *H. brachyrhynchus*. The sulcus endomarginalis that we identified in *H. crucians* was noted in *H. horridus* by Radinsky (1977) and appears to be more defined in the latter species. The line drawing of the endocast of *H. horridus* by Radinsky (1977:fig. 4) also features two very short successive sulci subdividing the broad gyrus above the sulcus rhinalis. These are not mentioned in the text but are faintly visible in the photographs in Saveliev and Lavrov (2001) and are similar to the sulcus ectosylvius we found in *H. crucians*. A similar sulcus was described in *H. brachyrhynchus* by Lange-Badré (1979). Saveliev and Lavrov (2001) noted a lozenge (a diamond-shape in the dorsal cerebrum similar to the ursine lozenge seen in some caniforms) in *H. horridus*, similar to that seen in *H. brachyrhynchus* (Lange-Badré, 1979), delimited by the sulcus cruciatus and sulcus precruciatus. The presence of this lozenge was not noted by Radinsky (1977) and cannot be confirmed or refuted by the photographs of Saveliev and Lavrov (2001).

Pterodon dasyuroides is represented by an imperfectly preserved natural endocast described by Piveteau (1935, 1961), Russel and Sigogneau (1965) and Radinsky (1977), and an artificial endocast by Lange-Badré (1979). Both Piveteau (1935) and Lange-Badré (1979) suggest that the midbrain was likely exposed, whereas Radinsky (1977) states that the edge of the neocortex reached the cerebellum and olfactory bulbs. After

Downloaded From: https://complete.bioone.org/journals/Journal-of-Vertebrate-Paleontology on 22 Mar 2025
Terms of Use: https://complete.bioone.org/terms-of-use

examining a digital rendering of the natural endocast, we are inclined to agree with Radinsky (1977). If there was midbrain exposure, it was to a much lesser extent than in, e.g., *Thinocyon velox* (Radinsky, 1977) and *Proviverra typica* (Dubied et al., 2019).

Comparison of Hyaenodont Endocasts

The brain morphology of *E. amorui* gen. et sp. nov. is similar to that of other known hyaenodonts. The degree of neocortical expansion is high compared to most earlier taxa, but similar to the contemporary *Megistotherium osteothlastes*. This is in spite of the nearly ten times greater endocast volume of the latter. *Megistotherium osteothlastes*, however, has an additional neocortical sulcus, the sulcus endomarginalis. Relative neocortex size and gyrification is influenced by the size of the brain (e.g., Jerison, 1973; Finlay and Darlington, 1995). The hyaenodonts most similar in brain size to *E. amorui* gen. et sp. nov. (40–41 ml) are *Tritemnodon agilis* (26 ml; Radinsky, 1977) and *Hyaenodon crucians* (47 ml; Radinsky, 1977). The neocortex of *T. agilis* (Radinsky, 1977) is much less expanded than that of *E. amorui* gen. et sp. nov. and lacks the sulcus suprasylvius. *Hyaenodon crucians* (Radinsky, 1977) displays a slightly lower degree of neocortical expansion than *E. amorui* gen. et sp. nov. but has a more elongated sulcus marginalis as well as a faint sulcus endomarginalis. Both *T. agilis* and *H. crucians* are notably older than *E. amorui* gen. et sp. nov., being early–middle Eocene and late Eocene–early Oligocene in age respectively.

The EQ of *E. amorui* gen. et sp. nov. is similar to that of most other hyaenodonts. Radinsky (1977) noted a trend of increasing EQ in Hyaenodonta, like in Carnivoramorpha. This conclusion was mainly based on the higher EQ of *Hyaenodon* spp. compared to older taxa. The geologically younger *E. amorui* gen. et sp. nov. and *M. osteothlastes* both have EQs that are more similar to the older taxa than to *Hyaenodon* spp., however, suggesting that this EQ increase was limited to the Hyaenodontidae. Nevertheless, the EQ is highly sensitive to the correct estimation of endocast volume and body mass, and several of these endocasts, including those of *E. amorui* gen. et sp. nov. and *M. osteothlastes*, are incomplete. Additionally, the body masses of different taxa have been estimated with different methods depending on the material available, leading to another potential source of error. It is therefore premature to draw any conclusions regarding evolutionary changes in EQ within Hyaenodonta.

Hyaenodonta display a great diversity in endocast morphology. Both Miocene species, *M. osteothlastes* and *E. amorui* gen. et sp. nov., are peculiar in that they display expanded neocortices and yet, as noted above, have similar EQ values to older, less neocorticalized taxa. Radinsky (1977) suggested that the low EQ of *M. osteothlastes* may result from the failure of the EQ equation (Jerison, 1973) to describe brain size scaling at very high body masses. This cannot account for the low EQ of *E. amorui* gen. et sp. nov., however, because it was a small animal. Nevertheless, the EQ of *E. amorui* gen. et sp. nov. is subject to significant error due to the underestimation of both endocast volume (due to incompleteness of the endocast) and body mass (due to the method of body mass estimation).

Paroxyaena pavlovi is also highly neocorticalized (Saveliev and Lavrov, 2007), but whether the expansion of the neocortex was associated with an increase in EQ in this species is unclear due to the uncertainty of the endocast volume (only cerebrum exposed) and body mass estimate (based on similarity in M1 size to a congeneric specimen). Even if the endocast volume and body mass of the individual could be accurately estimated, they may not be representative of the species, because the specimen in question is a juvenile with deciduous premolars in place (Lavrov, 2007). *Megistotherium osteothlastes* and *P. pavlovi* both share the sulcus endomarginalis. They also share the sulcus ectosylvius with *Pterodon dasyuroides*, suggesting that this sulcus is a shared feature among the Hyainailourinae. The sulcus ectosylvius is also present in *E. amorui* gen. et sp. nov., but not in *Apterodon macrognathus*, which may suggest the independent evolution of this sulcus within the Teratodontinae, or its loss in *A. macrognathus*.

Apterodon macrognathus (Radinsky, 1977) has a similar brain size to *P. pavlovi* but a somewhat less expanded neocortex. As previously noted by Radinsky (1977), *A. macrognathus* stands out with its distinctly arched sulci. Arching of the sulci is a distinctive feature of extant carnivorans, and Radinsky (1977) had two hypotheses for explaining this phenomenon: expansion of the auditory cortex, or packaging requirements in an expanding cortex. Nevertheless, he thought that neither of these hypotheses could explain the sulcal arching in *A. macrognathus*. The sulcal pattern could be related to the semiaquatic lifestyle recently suggested for *Apterodon* spp. (Frey et al., 2011; Grohé et al., 2012; Mahboubi et al., 2014). A study by Lyras et al. (2016) suggested that aquatic and semi-aquatic carnivorans as a rule have more gyrencephalic brains than terrestrial ones, but this is not the case with *A. macrognathus*. The homology between the functional regions of the cortex in hyaenodonts and carnivorans is currently not sufficiently established to speculate about more specific sensory adaptations such as those seen in the otter (Radinsky, 1968).

Apterodon macrognathus shares the sulcus suprasylvius with the hyainailourines and *E. amorui* gen. et sp. nov., but this sulcus is not found in *T. agilis* (nor any other hyaenodont, with the exception of *Hyaenodon* spp.), which is commonly recovered as a sister taxon to Hyainailouroidea (e.g., Borths et al., 2016; Borths and Stevens, 2019; Dubied et al., 2019). This may suggest that this sulcus is apomorphic to the Hyainailouroidea. With such a limited number of endocasts, of such varying morphology, however, the possibility of this sulcus arising several times within the clade cannot be disregarded. Curiously, one aspect of the morphology of this sulcus is shared by such diverse taxa as *M. osteothlastes*, *E. amorui* gen. et sp. nov. and *H. horridus*, namely that it curves medially at the anterior end to meet its counterpart of the other hemisphere, such that it can be seen as an indentation in the outline of the dorsal cerebrum in lateral aspect. This feature is less pronounced in *H. crucians* where the sulcus curves slightly medially but does not reach the fissura longitudinalis cerebri.

Among the Hyaenodontoidea, *Hyaenodon* species (e.g., Radinsky, 1977, Lange Badré, 1979) stand out with their relatively neocorticalized and gyrencephalic brains, as well as their high EQ. One possible explanation for the increased encephalization in *Hyaenodon* is a response to encephalization in prey species and competition with carnivoramorphs (Jerison, 1973), although this should have affected other hyaenodont taxa as well. It is possible that *Hyaenodon*, being hypercarnivorous (Mellett, 1977), competed with, and preyed on, different taxa than did the less specialized hyaenodont species. Many other factors have been correlated with increased encephalization in extant carnivorans, however, such as parental care (Gittleman, 1994), neonatal body mass and litter size (Finarelli, 2010), life span (Hofman, 1983), cognitive abilities (e.g., Benson-Amram et al., 2016), and sociality (Pérez-Barbería et al., 2007). The correlation between sociality and brain size in carnivorans has been repeatedly disputed, however (e.g., Finarelli and Flynn, 2009; Benson-Amram et al., 2016). A further complication is the fact that, as noted by Mellett (1977), the skull never stopped growing in *Hyaenodon*, and possibly neither did the body, though there is less material to prove this. Since the size of the brain case changed little throughout the adult life of the animal (Mellet, 1977:fig. 27), this means that the EQ should have decreased during its life span.

Downloaded From: https://complete.bioone.org/journals/Journal-of-Vertebrate-Paleontology on 22 Mar 2025
Terms of Use: https://complete.bioone.org/terms-of-use

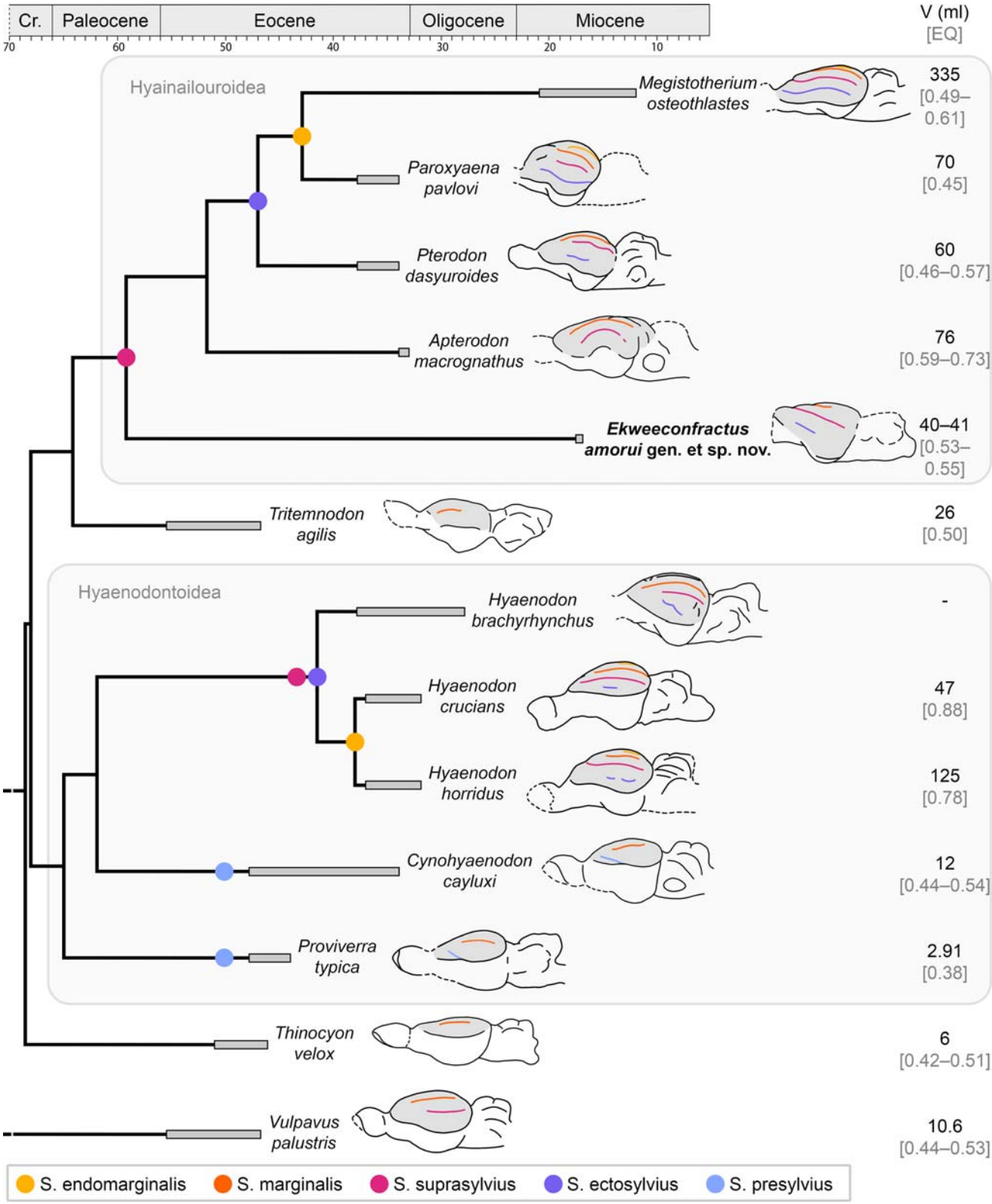

FIGURE 8. Phylogeny of taxa included in this study, with endocast drawings, volume (**V**, ml) and **EQ** (in brackets) for comparison. Phylogeny and divergence dates follow Dubied et al. (2019). Because *Hyaenodon brachyrhynchus* was not included in the phylogeny by Dubied et al. (2019), the divergence date for another European species, *H. exiguus*, was used instead. Age ranges of each species are listed in Supplemental Data 2. Endocast drawings, except that of *E. amorui* gen. et sp. nov., are based on descriptions by Radinsky (1977), Lange-Badré, (1979), Saveliev and Lavrov (2007) and Dubied et al. (2019) with the neocortex indicated in gray. The appearance of a sulcus within a clade is indicated by a colored circle. In the color version, different sulci are illustrated in corresponding colors on the endocasts. Endocast drawings are not to scale. **Abbreviation**: **Cr.**, Cretaceous.

Downloaded From: https://complete.bioone.org/journals/Journal-of-Vertebrate-Paleontology on 22 Mar 2025
Terms of Use: https://complete.bioone.org/terms-of-use

The basal hyaenodontid *C. cayluxi* (Borths et al., 2016; Borths and Stevens, 2019; Dubied et al., 2019) displays a low degree of neocorticalization compared to its younger, larger confamilials of the genus *Hyaenodon* (Radinsky, 1977). This further supports the notion that the expansion and gyrification of the neocortex, and acquisition of the sulcus suprasylvius, occurred convergently within Hyaenodontoidea and Hyainailouroidea. *Proviverra typica* (Dubied et al., 2019) displays numerous similarities in neocortical morphology to *C. cayluxi* (Radinsky, 1977), such as a similar degree of neocortical expansion, and the presence of a sulcus presylvius. The phylogenetic position of *P. typica* is uncertain (e.g., Borths et al., 2016), but in the recent phylogeny by Dubied et al. (2019) it was included in Hyaenodontoidea (Fig. 8). This placement is in agreement with the neocortical morphology.

Thinocyon velox is the hyaenodont studied herein that displays the lowest degree of neocortical expansion (Fig. 8). Radinsky (1977) also suggested a low degree of neocortical expansion for another limnocyonine, *Oxyaenodon* sp., based on a partial natural endocast. Limnocyoninae are placed basally within Hyaenodonta in recent phylogenetic studies (e.g., Borths and Stevens, 2019; Dubied et al., 2019). This, together with the relatively low degree of neocorticalization in *T. agilis*, *P. typica* and *C. cayluxi*, suggests that the first hyaenodonts had relatively small neocortices and that increasing neocorticalization and gyrification occurred independently in Hyaenodontoidea and Hyainailouroidea. Borths et al. (2016) recovered Limnocyoninae as the sister group of the clade containing *T. agilis* and Hyainailouroidea when using strict, Adams, and standard Bayesian consensus trees (Borths et al., 2016:figs. 17, 18, 20, 21). Nevertheless, this has little impact on the results herein, because the endocasts of *C. cayluxi* and *P. typica* still point towards a low degree of neocorticalization and gyrification in the first hyaenodontids, and thus the first hyaenodonts. As we shall see below, the endocast morphology of oxyaenids (Radinsky, 1977; Ahrens and Passero, 2019) and an early carnivoramorph (Radinsky, 1977) also support a relatively small neocortex in the first hyaenodonts. Additionally, *P. typica* was recovered basally within Hyaenodonta by Borths and Stevens (2019) and Borths et al. (2016: figs. 18, 19, 21, 22) when using standard Bayesian or Bayesian tip-dating analysis. In this case the relatively small neocortex of this species also supports the hypothesis of a low degree of neocortical expansion in the first hyaenodonts.

The oldest known hyaenodont endocasts, such as *T. velox* and *T. agilis*, indicate a degree of neocortical expansion similar to the late Paleocene oxyaenid *Dipsalidictis krausei* (Ahrens and Passero, 2019). The digital endocast of *D. krausei* is so far only described in an abstract and is the only complete oxyaenid endocast described to date (Ahrens and Passero, 2019). Based on more fragmentary material, Radinsky (1977) also suggested a low degree of neocorticalization in the early Eocene *Oxyaena* sp. and middle Eocene *Patriofelis ulta* (Wortman, 1894; Denison, 1938).

The oldest known carnivoramorph endocast, of the late Paleocene viverravid *Didymictis*, is crushed, but was described by Radinsky (1977) as indicating a low degree of neocortical expansion with no evidence of neocortical sulci. Radinsky (1977) also described an endocast of the Eocene carnivoraform *Vulpavus palustris*, which appears to be the oldest nearly complete carnivoramorph endocast that has been figured in the literature. It was included in Table 1 and Fig. 8 for comparison with hyaenodonts. This endocast was described by Radinsky (1977) as displaying considerably more neocortical expansion than that of *Didymictis*, with a nearly completely covered midbrain and two neocortical sulci. An undistorted, complete digital endocast of the closely related *Oodectes herpestoides* was described in an abstract by Spaulding and Flynn (2012). They noted many similarities with *V. palustris* but also that the frontal pole of the neocortex was slightly more expanded in *O. herpestoides*, so that it reached the olfactory bulbs. The endocast morphologies of *V. palustris* and *O. herpestoides* suggest a greater degree of neocorticalization in early Eocene carnivoramorphs than in contemporary hyaenodonts, even if absolute size is taken into account. The endocast volume of *V. palustris* is 10.6 ml compared to 6 ml and 26 ml in *T. velox* and *T. agilis*, respectively (Radinsky, 1977). The late Eocene carnivoraform *Quercygale angustidens* has a larger brain (20.5 ml) and a more expanded neocortex than *V. palustris*, with longer sulci (*Procynodictis angustidens* in Radinsky, 1977). *Quercygale angustidens* appears to display a degree of neocortical expansion most similar to the contemporary, but larger, *Hyaenodon brachyrhynchus* (Lange-Badré, 1979) among the hyaenodonts.

CONCLUSIONS

Radinsky (1977) noted the increasing neocorticalization through time in Hyaenodonta. This trend is further highlighted by the additional specimens described since then (Lange-Badré, 1979; Saveliev and Lavrov, 2007; Dubied et al., 2019), and most notably by *E. amorui* gen. et sp. nov. which adds a neocorticalized Miocene species of relatively small body size to the record of hyaenodont endocasts. When accounting for the phylogenetic relationships within the order it appears that this expansion of the neocortex and acquisition of additional sulci occurred convergently within Hyaenodontoidea and Hyainailouroidea. This is not surprising considering that these clades are thought to have originated in the Paleocene or even earlier (e.g., Borths and Stevens, 2019), and all taxa in this study are of Eocene age or younger. What may be surprising, however, is that the expansion of the neocortex may not have been accompanied by an increase in relative brain size (EQ) in Hyainailouroidea. This suggests that the expansion of the neocortex occurred at the expense of other parts of the brain in this group. However, as noted above, many endocasts are incomplete and their full volume is uncertain. Likewise, the body mass estimates are uncertain because different methods of body mass estimation are used for different specimens depending on which parts of the skeleton are preserved.

Although many studies have focused on the evolution of the brain in recent mammalian carnivores, or extinct members of extant carnivore families (e.g., Lyras and van der Geer, 2003; Lyras, 2009; Lyras et al., 2016), little is known about the brains of the members of extinct clades such as Hyaenodonta, Oxyaenidae, Viverravidae and basal carnivoraforms ('Miacidae'). This is largely due to the paucity of suitable specimens of the latter groups. The advent of 3D technology, however, is leading to an increase in specimens in the form of digital endocasts (e.g., Ahrens and Passero, 2019; Dubied et al., 2019). It also allows for the digitization of physical endocasts, which makes these specimens more widely accessible and allows for digital measurements. A larger number of more complete endocasts would allow for more thorough studies of increasing gyrification through time, similar to the study on carnivorans by Lyras et al. (2016), and for testing of phylogenetic signal in endocast morphology (cf. Ahrens, 2014). Such studies have the potential to greatly increase our understanding of the evolution of the brain in Hyaenodonta, and more generally, in mammals as a whole.

ACKNOWLEDGMENTS

The authors thank K. Jakata at the Evolutionary Studies Institute, University of the Witwatersrand, for assisting with the scanning of the specimen and G. A. Lyras for providing 3D models of several fossil endocasts for comparison. We

Downloaded From: https://complete.bioone.org/journals/Journal-of-Vertebrate-Paleontology on 22 Mar 2025
Terms of Use: https://complete.bioone.org/terms-of-use

particularly thank W. Lukens for his careful analysis of the depositional settings in the Moruorot excavation. We are grateful to C. Kiare for his expert preparation and to M. Leakey for hand-delivering the specimen from Turkana to the National Museum in Nairobi. Furthermore, this project would not have been possible without the West Turkana Research Project and all the people involved in it at all levels and tasks. This project forms part of the NSF-funded Research on East African Catarrhine and Hominoid Evolution (REACHE) Project and is REACHE Paper #16. Fieldwork by The West Turkana Miocene Project was funded by NSF award BCS 1241817 to JBR, the Natural Sciences and Engineering Research Council of Canada, and the University of Calgary.

LITERATURE CITED

Ahrens, H. E. 2014. Morphometric study of phylogenetic and ecologic signals in procyonid (Mammalia: Carnivora) endocasts. Anatomical Record 297:2318–2330.

Ahrens, H. E., and M. Passero. 2019. Endocast of the Paleocene carnivore *Dipsalidictis krausei* (Mammalia, Creodonta). The FASEB Journal 33:614.4.

Arambourg, C. 1933. Mammifères Miocènes de Turkana (Afrique Orientale). Annales de Paléontologie 22:123–146.

Arambourg, C. 1944. Contribution a l'étude géologique et paléontologique du Bassin du Lac Rodolphe et de la Basse Vallée de L'Omo. Première Partie: Géologie; pp. 157–230 in C. Arambourg (ed.), Mission Scientifique de L'Omo. Muséum National d'Histoire Naturelle, Paris.

Bajpai, S., V. V. Kapur, and J. G. M. Thewissen. 2009. Creodont and condylarth from the Cambay Shale (early Eocene, 55–54 Ma), Vastan Lignite Mine, Gujarat, Western India. Journal of the Palaeontological Society of India 54:103–109.

Bartley, A. J., D. W. Jones, and D. R. Weinberger. 1997. Genetic variability of human brain size and cortical gyral patterns. Brain 120:257–269.

Benson-Amram, S., B. Dantzer, G. Stricker, E. M. Swanson, and K. E. Holekamp. 2016. Brain size predicts problem-solving ability in mammalian carnivores. Proceedings of the National Academy of Sciences 113:2532–2537.

Borths, M. R., and E. R. Seiffert. 2017. Craniodental and humeral morphology of a new species of *Masrasector* (Teratodontinae, Hyaenodonta, Placentalia) from the late Eocene of Egypt and locomotor diversity in hyaenodonts. PLOS One 12:e0173527.

Borths, M. R., and N. J. Stevens. 2017. The first hyaenodont from the late Oligocene Nsungwe Formation of Tanzania: Paleoecological insights into the Paleogene–Neogene carnivore transition. PLoS ONE 12:1–30.

Borths, M. R., and N. J. Stevens. 2019. *Simbakubwa kutokaafrika*, gen. et sp. nov. (Hyainailourinae, Hyaenodonta, 'Creodonta,' Mammalia), a gigantic carnivore from the earliest Miocene of Kenya. Journal of Vertebrate Paleontology: e1570222.

Borths, M. R., P. A. Holroyd, and E. R. Seiffert. 2016. Hyainailourine and teratodontine cranial material from the late Eocene of Egypt and the application of parsimony and Bayesian methods to the phylogeny and biogeography of Hyaenodonta (Placentalia, Mammalia). PeerJ 4:e2639.

Boschetto, H. B., F. H. Brown, and I. McDougall. 1992. Stratigraphy of the Lothidok Range, northern Kenya, and K/Ar ages of its Miocene primates. Journal of Human Evolution 22:47–71.

Cote, S., J. Kingston, A. Deino, A. Winkler, R. Kityo, and L. MacLatchy. 2018. Evidence for rapid faunal change in the early Miocene of East Africa based on revised biostratigraphic and radiometric dating of Bukwa, Uganda. Journal of Human Evolution 116:95–107.

Crochet, J.-Y., S. Peigné, and M. Mahboubi. 2001. Ancienneté des Carnivora (Mammalia) en Afrique.; pp. 91–100 in C. Denys, L. Granjon, and A. Poulet (eds.), African Small Mammals. Petits mammifères africains. IRD Publishers, Paris.

Crochet, J.-Y., H. Thomas, J. Roger, and S. Al-Sulaimani. 1990. Première découverte d'un créodonte dans la péninsule Arabique: *Masrasector ligabuei* nov. sp. (Oligocène inférieur de Taqah, Formation d'Ashawq, Sultanat d'Oman. Comptes Rendus de l'Académie des Sciences II 311:1455–1460.

Cuvier, G. 1804. Sur les espèces d'animaux dont provennient les os fossiles répandus dans la pierre à plâtre des environs de Paris. Annales du Muséum d'Histoire Naturelle 3:275–303.

Denison, R. H. 1938. The broad-skulled Pseudocreodi. Annals of the New York Academy of Sciences 37:163–257.

Drake, R. E., J. A. Van Couvering, M. Pickford, G. H. Curtis, J. A. Harris. 1988. New chronology for the early Miocene mammalian faunas of Kisingiri, western Kenya. Journal of the Geological Society 145:479–491.

Dubied, M., F. Solé, B. Mennecart, and L. Hautier. 2019. The cranium of *Proviverra typica* (Mammalia, Hyaenodonta) and its impact on hyaenodont phylogeny and endocranial evolution. Palaeontology 62:983–1001.

Edinger, T. 1931. Zwei Schädelhöhlen-Steinkerne von *Pannonictis pliocaenica* Kormos. Annales Instituti Regii Hungarici Geologici 29:179–184.

Edinger, T. 1975. Paleoneurology 1804–1966. An annotated bibliography. Advances in Anatomy, Embryology and Cell Biology 49:7–258.

Eisenberg, J. F. 1981. The Mammalian Radiations: An Analysis of Trends in Evolution, Adaptation, and Behavior. University of Chicago Press, 610 pp.

Filhol, H. 1877. Recherches sur les phosphorites du Quercy. Étude des fossiles qu'on y rencontre. Annales des Sciences Géologiques 8:1–340.

Finarelli, J. A. 2010. Does encephalization correlate with life history or metabolic rate in carnivora? Biology Letters 6:350–353.

Finarelli, J. A., and J. J. Flynn. 2009. Brain-size evolution and sociality in Carnivora. Proceedings of the National Academy of Sciences of the United States of America 106:9345–9349.

Finlay, B. L., and R. B. Darlington. 1995. Linked regularities in the development and evolution of mammalian brains. Science 268:1578–1584.

Flynn, J. J., and G. D. Wesley-Hunt. 2005. Carnivora; pp. 175–198 in K. D. Rose and J. D. Archibald (eds.), The Rise of Placental mammals: Origins and Relationships of the Major Extant Clades. The Johns Hopkins University Press, Baltimore.

Frey, E., W. Munk, M. Böhme, M. Morlo, and M. Hensel. 2011. First creodont carnivore from the Rupelian Clays (Oligocene) of the Clay Pit Unterfeld at Rauenberg (Rhein-Neckar-Kreis, Baden Württemberg): *Apterodon rauenbergensis*, n.sp. Kaupia 17:107–113.

Friscia, A. R., and B. van Valkenburgh. 2010. Ecomorphology of North American Eocene carnivores: evidence for competition between carnivorans and creodonts; pp. 311–341 in A. Goswami and A. Friscia (eds.), Carnivoran Evolution. New Views on Phylogeny, Form, and Function. Cambridge University Press, Cambridge.

Gaudry, A. 1878. Les Enchainements du Monde Animal dans les Temps Géologiques: Mammifères Tertiaires. Librairie Hachette et C., Paris, 293 pp.

Gervais, P. 1870. Mémoire sur les formes cérébrales propres aux carnivores vivants et fossiles. Nouvelles Archives du Muséum d'Histoire Naturelle de Paris 6:103–162.

Gittleman, J. L. 1994. Female brain size and parental care in carnivores. Proceedings of the National Academy of Sciences of the United States of America 91:5495–5497.

Goloboff, P. A., J. S. Farris, and K. C. Nixon. 2008. TNT, a free program for phylogenetic analysis. Cladistics 24:774–786.

Grohé, C., M. Morlo, Y. Chaimanee, C. Blondel, P. Coster, X. Valentin, M. Salem, A. A. Bilal, J.-J. Jaeger, and M. Brunet. 2012. New Apterodontinae (Hyaenodontida) from the Eocene locality of Dur At-Talah (Libya): Systematic, Paleoecological and Phylogenetical Implications. PLoS ONE 7.

Heuer, K., and R. Toro. 2019. Role of mechanical morphogenesis in the development and evolution of the neocortex. Physics of Life Reviews 31:233–239.

Hofman, M. A. 1983. Energy metabolism, brain size and longevity in mammals. The Quarterly Review of Biology 58:495–512.

Jerison, H. J. 1969. Brain evolution and dinosaur brains. The American Naturalist 103:575–588.

Jerison, H. J. 1973. Evolution of the Brain and Intelligence. Academic Press, New York, 482 pp.

Kaas, J. H. 2016. The organization of neocortex in early mammals; pp. 87–101 in J. H. Kaas (ed.), Evolution of Nervous Systems, 2nd Edition, Volume 2. Elsevier Science & Technology, San Diego.

Klinghardt, F. 1934. Gerhirnrelief und Schädelstudien über *Hyaenodon* und *Dinictis*. Zeitschrift für Säugetierkunde 9:76–86.

Downloaded From: https://complete.bioone.org/journals/Journal-of-Vertebrate-Paleontology on 22 Mar 2025
Terms of Use: https://complete.bioone.org/terms-of-use

Lange-Badré, B. 1979. Les créodontes (Mammalia) d'Europe occidentale de l'Éocène supérieur à l'Oligocène supérieur. Mémoires du Muséum National d'Histoire Naturelle N. S., sér. C, 42:1–249.

Lavrov, A. V. 2007. A new species of *Paroxyaena* (Hyaenodontidae, Creodonta) from phosphorites of Quercy, Late Eocene, France. Paleontological Journal 41:298–311.

Leakey, M., A. Grossman, M. Gutierrez, and J. G. Fleagle. 2011. Faunal change in the Turkana Basin during the late Oligocene and Miocene. Evolutionary Anthropology 20:238–53.

Leidy, J. 1869. The extinct mammalian fauna of Dakota and Nebraska including an account of some allied forms from other localities, together with a synopsis of the mammalian remains of North America. Journal of the Academy of Natural Sciences of Philadelphia 2nd Series 7:1–472.

López-Torres, S., O. C. Bertrand, M. M. Lang, M. T. Silcox, and Ł. Fostowicz-Frelik. 2020. Cranial endocast of the stem lagomorph *Megalagus* and brain structure of basal Euarchontoglires. Proceedings of the Royal Society B 287:20200665.

Lyras, G. A. 2009. The evolution of the brain in Canidae. Scripta Geologica 139:1–93.

Lyras, G. A., and A. A. E. van der Geer. 2003. External brain anatomy in relation to phylogeny of Caninae (Carnivora: Canidae). Zoological Journal of the Linnean Society 138:505–522.

Lyras, G. A., A. Giannakopoulou, M. Kouvari, and G. C. Papadopoulos. 2016. Evolution of gyrification in carnivores. Brain, Behavior and Evolution 88:187–203.

Maddison, W. P. and D.R. Maddison. 2019. Mesquite: a modular system for evolutionary analysis. Version 3.61 http://www.mesquiteproject.org.

Mahboubi, S., H. Bocherens, M. Scheffler, M. Benammi, and J.-J. Jaeger. 2014. Was the early Eocene proboscidean *Numidotherium koholense* semi-aquatic or terrestrial? Evidence from stable isotopes and bone histology. Comptes Rendus Palevol 13:501–509.

Mellet, J. S. 1977. Paleobiology of North American *Hyaenodon* (Mammalia, Creodonta); in M. K. Hecht and F. S. Szalay (eds.), Contributions to Vertebrate Evolution, Volume 1. Karger, New York, 134 pp.

Morlo, M. 1999. Niche structure and evolution in creodont (Mammalia) faunas of the European and North American Eocene. Geobios 32:297–305.

Pérez-Barbería, F. J., S. Shultz, and R. I. M. Dunbar. 2007. Evidence for coevolution of sociality and relative brain size in three orders of mammals. Evolution 61:2811–2821.

Pilgrim, G. E. 1932. The fossil carnivora of India. Memoirs of the Geological Survey of India. Paleontologica Indica 18:1–232.

Piveteau, J. 1935. Études sur quelques créodontes des phosphorites du Quercy. Annales de Paléontologie 24:75–95.

Piveteau, J. 1951. Recherches sur l'évolution de l'encéphale chez les carnivores fossiles. Annales de Paléontologie 37:136–151.

Piveteau, J. 1961. Encéphales de carnivores fossiles; pp. 806–820 in J. Piveteau (ed.), Traité de Paléontologie. Masson, Paris.

Radinsky, L. 1968. Evolution of somatic sensory specialization in otter brains. Journal of Comparative Neurology 134:495–506.

Radinsky, L. 1969. Outlines of canid and felid brain evolution. Annals of the New York Academy of Sciences 167:277–292.

Radinsky, L. 1973. Evolution of the canid brain. Brain, behavior and evolution 7:169–202.

Radinsky, L. 1975. Evolution of the felid brain. Brain, behavior and evolution 11:214–254.

Radinsky, L. 1977. Brains of early carnivores. Paleobiology 3:333–349.

Radinsky, L. 1978. Evolution of brain size in carnivores and ungulates. The American Naturalist 112:815–831.

Rana, R. S., K. Kumar, S. P. Zack, F. Solé, K. D. Rose, P. Missiaen, L. Singh, A. Sahni, and T. Smith. 2015. Craniodental and postcranial morphology of *Indohyaenodon raoi* from the early Eocene of India, and its implications for ecology, phylogeny, and biogeography of hyaenodontid mammals. Journal of Vertebrate Paleontology 35: e965308.

Rossie, J. B., and S. Cote. 2017. New material of *Turkanapithecus* and *Simiolus* from West Turkana, Kenya. American Journal of Physical Anthropology Supplement 162:337.

Rossie, J. B., M. M. Gutierrez, and E. Goble. 2012. Fossil forelimbs of *Simiolus* from Moruorot, Kenya. American Journal of Physical Anthropology Supplement 54:252.

Russel, D. E., and D. Sigogneau. 1965. Étude des moulages endocrâniens de Mammifères Paléocènes. Memoires du Museum National d'Histoire Naturelle Sér. C 16:1–35.

Savage, R. J. G. 1965. Fossil mammals of Africa: 19. The Miocene Carnivora of East Africa. Bulletin of the British Museum (Natural History) Geology 10:239–316.

Savage, R. J. G. 1973. *Megistotherium*, gigantic hyaenodont from Miocene of Gebel Zelten, Libya. Bulletin of the British Museum (Natural History), Geology 22:483–511.

Saveliev, S. V., and A. V. Lavrov. 2001. A morpho-functional reconstruction of the brain of *Neohyaenodon horridus* (Hyaenodontidae, Creodonta) based on a natural endocranial cast. Paleontological Journal 35:75–83.

Saveliev, S. V., and A. V. Lavrov. 2007. Morphofunctional reconstruction of the brain of *Paroxyaena pavlovi* (Hyaenodontidae, Creodonta) based on a natural endocranial cast. Paleontological Journal 41:661–670.

Scott, W. B. 1888. On some new and little-known creodonts. Journal of the Academy of Natural Sciences of Philadelphia 2nd series, Vol. 2:155–185.

Simons, E. L., and P. D. Gingerich. 1974. New carnivorous mammals from the Oligocene of Egypt. Annals of the Geological Survey of Egypt 4:157–166.

Solé, F., J. Falconnet, D. Vidalenc, and A. Goswami. 2015a. New fossil Hyaenodonta (Mammalia, Placentalia) from the Ypresian and Lutetian of France and the evolution of the Proviverrinae in southern Europe. Palaeontology 58:1049–1072.

Solé, F., E. Amson, M. Borths, D. Vidalenc, M. Morlo, and K. Bastl. 2015b. A new large hyainailourine from the Bartonian of Europe and its bearings on the evolution and ecology of massive hyaenodonts (Mammalia). PLOS One 10:e0135698.

Solé, F., J. Lhuillier, M. Adaci, M. Bensalah, M. Mahboubi, and R. Tabuce. 2014. The hyaenodontidans from the Gour Lazib area (?Early Eocene, Algeria): implications concerning the systematics and the origin of the Hyainailourinae and Teratodontinae. Journal of Systematic Palaeontology 12:303–322.

Spaulding, M., and J. J. Flynn. 2012. A virtual endocast and endocranial features of *Oodectes* (Mammalia: Carnivoramorpha). Journal of Vertebrate Paleontology 32:177–177.

Spaulding, M., M. A. O'Leary, and J. Gatesy. 2009. Relationships of Cetacea (Artiodactyla) among mammals: increased taxon sampling alters interpretations of key fossils and character evolution. PLOS One 4:e7062.

Toro, R. 2012. On the possible shapes of the brain. Evolutionary Biology 39:600–612.

Van Valen, L. 1967. New Paleocene insectivores and insectivore classification. Bulletin of the American Museum of Natural History 135:217–284.

Van Valkenburgh, B. 1990. Skeletal and dental predictors of body mass in carnivores; pp. 181–206 in J. Damuth and B. J. MacFadden (eds.), Body size in mammalian paleobiology: Estimation and biological implications. Cambridge University Press.

Welker, W. I., and G. B. Campos. 1963. Physiological significance of sulci in somatic sensory cerebral cortex in mammals of the family Procyonidae. Journal of Comparative Neurology 120:19–36.

Wortman, J. L. 1894. Osteology of *Patriofelis*, a middle Eocene creodont. Bulletin of the American Museum of Natural History 6:129–164.

World Association of Veterinary Anatomists. 2017. Nomina Anatomica Veterinaria. International Committee on Veterinary Gross Anatomical Nomenclature. Editorial Committee, Hannover (Germany), Ghent (Belgium), Columbia, Missouri (U.S.A.), Río de Janeiro (Brazil), 160 pp.

Submitted March 23, 2020; revisions received April 11, 2021;
accepted April 13, 2021.
Handling Editor: Matthew Borths.

Downloaded From: https://complete.bioone.org/journals/Journal-of-Vertebrate-Paleontology on 22 Mar 2025
Terms of Use: https://complete.bioone.org/terms-of-use